Characterizing and Forecasting climate indices using time series models

Taesam Lee[1], Taha B.M.J. Ouarda[2] and Ousmane Seidou[3]

[1]Department of Civil Engineering, ERI, Gyeongsang National University

501 Jinju-daero, Jinju, 52828, South Korea

[2]Canada Research Chair in Statistical Hydro-Climatology, INRS-ETE 490, de la Couronne

Québec (Québec) G1K 9A9, CANADA

[3]Dept. of Civil Engineering, University of Ottawa

161 Louis Pasteur Office A113, Ottawa, ON, K1N 6N5, CANADA

Corresponding Author: Taesam Lee, Department of Civil Engineering, Gyeongsang National University, ERI, 501 Jinju-daero, Jinju, Gyeongsangnam-do, 660-701, South Korea, E-mail: tae3lee@gnu.ac.kr, Tel: +82 55 772 1797

Abstract

The objective of the current study is to present a comparison of techniques for the forecasting of low frequency climate oscillation indices with a focus on the Great Lakes system. A number of time series models have been tested including the traditional Autoregressive Moving Average (ARMA) model, Dynamic Linear model (DLM), Generalized Autoregressive Conditional Heteroskedasticity (GARCH) model, as well as the nonstationary oscillation resampling (NSOR) technique. These models were used to forecast the monthly El Niño-Southern Oscillation (ENSO) and Pacific Decadal Oscillation (PDO) indices which show the most significant teleconnection with the net basin supply (NBS) of the Great Lakes system from a preliminary study. The overall objective is to predict future water levels, ice extent, and temperature, for planning and decision making purposes. The results showed that the DLM and GARCH models are superior for forecasting the monthly ENSO index, while the forecasted values from the traditional ARMA model presented a good agreement with the observed values within a short lead time ahead for the monthly PDO index.

Keywords: ARMA, Climate Index, Dynamic Linear Model, ENSO, GARCH, PDO, Time Series

1. Introduction

It is well established that low frequency Climate oscillation indices such as the El Niño-Southern Oscillation (ENSO) (Tsonis et al., 2007), and the Pacific Decadal Oscillation (PDO) (Mantua et al., 1997) indices are related to hydro-meteorological variables in a number of regions of the globe (Ouachani et al., 2013, Naizghi and Ouarda, 2017, Niranjan Kumar et al., 2016). Such relations are termed as ‘teleconnections’ (Alexander et al., 2002, Burg, 1978, Kalman, 1960, Ouachani et al., 2013, Schneider et al., 1999). For example, Rodionov and Assel (2003) found that a substantial difference of the large-scale atmospheric circulation associated with the ENSO and PDO leads to an abnormally mild winter in the Great Lakes region.

Therefore, these climate indices have been identified as remarkably good predictors of hydro-meteorological variables (Cheng et al., 2010a, Immerzeel and Bierkens, 2010, Schneider et al., 1999, Thomas, 2007, Westra and Sharma, 2010). A number of methods have been developed to forecast climate indices (Chen et al., 2004, Cheng et al., 2010a, Cheng et al., 2010b). These are mainly based on Global Climate Models (GCM) (Kirtman and Min, 2009, Schneider et al., 1999, Wu and Kirtman, 2003). However, GCM based forecasting is rather expensive, and is not always available beyond the atmospheric research community. In the current study, we propose to forecast climate indices based on time series models which are much cheaper and easier to implement than GCM-based models.

The traditional autoregressive moving average (ARMA) time series model (Brockwell and Davis, 2003), the Dynamic Linear Model (DLM) (West and Harrison, 1997, Petris et al., 2009), the Generalized Autoregressive Conditionally Heteroscedastic (GARCH) model (Engle, 1982, Modarres and Ouarda, 2013a, Modarres and Ouarda, 2013b, Modarres and Ouarda, 2014) as well as the NonStationary Oscillation Resampling (NSOR) technique developed by Lee and Ouarda (2011b) are employed to forecast climate indices. Nonlinear time series models (Fan and Yao, 2003, Ahn and Kim, 2005) were also considered and omitted since we found that no significant nonlinear serial dependences are present in the considered climate indices.

The scientific literature, and a preliminary study that we carried out confirmed that the NBS components of the Great Lakes can be better forecasted by incorporating the teleconnections with the forecasted climate index, especially in the case of ENSO. Thus, the primary objective of the current study is to forecast these monthly climate indices using time series models in order to incorporate them in the prediction of the NBS components of the Great Lakes system.

In section 2, the introduction and mathematical description of the applied time series models are presented. The employed climate indices are explained in section 3. The performance and skills of the forecasted climate indices of ENSO and PDO are discussed in section 4 and section 5, respectively. Summary and conclusions are presented in section 6.

2. Mathematical description of applied models

2.1. ARMA

2.1.1. Model Description

Let us assume X_t to be an ARMA(p, q) process. if X_t is stationary we have for every t:

$$X_t - \phi_1 X_{t-1} - \ldots - \phi_p X_{t-p} = Z_t + \theta_1 Z_{t-1} + \ldots + \theta_q Z_{t-q} \quad (1)$$

where Z_t is a white noise with zero mean (i.e. $\mu_Z = 0$) and variance σ_Z^2 (Brockwell and Davis, 2003, Salas et al., 1980). X_t is said to be an ARMA(p, q) process with mean μ_X if $X_t - \mu_X$ is an ARMA(p, q) process. Simply, Eq.(1) is also expressed as:

$$\phi(B) X_t = \theta(B) Z_t \quad (2)$$

where $\phi(B) = 1 - \phi_1 B - \ldots - \phi_p B^p$ and $\theta(B) = 1 + \theta_1 B + \ldots + \theta_q B^q$ and B is the backward shift operator. X_t in Eq.(2) is further expressed as:

$$X_t = \frac{\theta(B)}{\phi(B)} Z_t = \psi(B) Z_t = \sum_{j=0}^{\infty} \psi_j Z_{t-j} \quad (3)$$

where $\psi(B) = \dfrac{\theta(B)}{\phi(B)}$.

2.1.2. Parameter estimation and model selection

A number of methods to estimate the parameters of the ARMA process in Eq.(1) have been developed such as Yule-Walker estimation (Yule, 1927, Walker, 1932), Burg's algorithm based on the forward and backward prediction errors (Burg, 1978), the innovations algorithms (Brockwell and Davis, 1988), Hannan-Rissanen algorithm (Hannan and Rissanen, 1982), and maximum likelihood estimation (MLE)(Brockwell and Davis, 2003).

The Yule-Walker estimation is derived by multiplying each side of Eq.(1) by X_{t-j} , j=0,1,…, p+q and taking the expectation. These relations of the lagged second moments (auto-covariance) up to p+q are called the Yule-Walker equation. The p+q+1 Yule-Walker equations are solved using the sample lagged second moments to estimate the parameters of the ARMA model.

In MLE, supposing that X_t is a Gaussian time series, the likelihood of $\mathbf{X}_n = (X_1,\ldots,X_n)'$, where n is the number of records, is maximized to estimate the parameters:

$$L(\boldsymbol{\psi}) = (2\pi)^{-2n} \det(\mathbf{C}_n)^{-1/2} \exp(-1/2\mathbf{X}_n{}'\mathbf{C}_n{}^{-1}\mathbf{X}_n) \quad (4)$$

where $\mathbf{C}_n = E(\mathbf{X}_n{}'\mathbf{X}_n)$, $\boldsymbol{\psi} = [\boldsymbol{\varphi}, \boldsymbol{\theta}, \sigma_Z^2]$ and $\boldsymbol{\varphi} = (\phi_1,\ldots,\phi_p)'$, $\boldsymbol{\theta} = (\theta_1,\ldots,\theta_q)'$ and the prime (') implies the transpose. Note that the right side of Eq.(4) can be described as the function of $\boldsymbol{\varphi}$, $\boldsymbol{\theta}$, and σ_Z^2 (Brockwell and Davis, 2003). MLE was used to estimate the parameters of the ARMA model in the current study.

The Akaike Information Criterion (AIC) was proposed by Akaike (1974) to compare models with a different number of parameters so that one can select the best model with the lowest AIC value. The criterion is written as:

$$\mathrm{AIC} = 2n_{par} - 2\log(L(\boldsymbol{\psi})) \quad (5)$$

where n_{par} is the number of parameters. Hurvich and Tsai (1989) introduced the bias corrected version of AIC, AICC, defined as:

$$\mathrm{AICC} = \mathrm{AIC} + 2n_{par}(n_{par}+1)/(n-n_{par}-1) \quad (6)$$

2.1.3. Forecasting ARMA process

Forecasting X_{n+h} , $h>0$ with the available data up to n is to find the linear combination of [X_n , X_{n-1} ,…, X_1] with minimum mean squared error where h is the lead time. The h-step ahead forecast X_{n+h} is:

$$\hat{X}_n(h) = \phi_1[X_{n+h-1}] + \ldots + \phi_p[X_{n+h-p}] - \theta_1[Z_{n+h-1}] - \ldots - \theta_1[Z_{n+h-q}] \quad (7)$$

For quantities inside [], substitute the value if known, forecast if unknown as $\hat{X}_n(h-k)$ for X_{n+h-k}, and 0 for Z_{n+h-k} where k=1,…,h-1. Further complete the process of the forecasting ARMA process is referred to in Brockwell and Davis (2003).

2.2.GARCH

Engle (1982) introduced Autoregressive conditional heteroscedastic (ARCH) models to generalize the assumption of a constant one-period forecast variance. Their GARCH (generalized ARCH) extension is due to Bollerslev (1986). The fundamental concept of the GARCH is that the current value of the variance is dependent on the past values. Thus, the conditional variance is expressed as a linear function of the squared past values of the series (Engle and Kroner, 1995). GARCH has been widely used in Econometrics, climatology, health sciences and other fields (Engle, 2002, Engle, 2001, Bosley et al., 2008, Bollerslev et al., 1992). Applications in the hydrometeorological field are relatively limited and include the work of Elek and Márkus (2004), Ahn and Kim (2005), Wang et al. (2005), and Modarres and Ouarda (2014). The brief definition of GARCH and its forecasting procedure is presented in the following subsections.

2.2.1. Definitions and representations of GARCH($\tilde{p},\tilde{q}$)

A process Z_t is called GARCH($\tilde{p},\tilde{q}$) process if satisfying the following :

(i) $E(Z_t \mid Z_u, u<t) = 0$ (8)

(ii) $\sigma_t^2 = Var(Z_t \mid Z_u, u<t) = \omega + \alpha(B)Z_t^2 + \beta(B)\sigma_t^2$ (9)

where, the parameters of the GARCH process (ω, $\alpha(B) = \sum_{i=1}^{\tilde{q}} \alpha_i B^i$ and $\beta(B) = \sum_{i=1}^{\tilde{p}} \beta_i B^i$) exist.

The likelihood of the GARCH process is:

$$L(\boldsymbol{\psi}) = \prod_{t=1}^{n} (2\pi\sigma_t^2)^{-1/2} \exp\left(-\frac{Z_t^2}{\sigma_t^2}\right) \tag{10}$$

where $\boldsymbol{\psi}$ are all the parameters of the GARCH process. These parameters are estimated by MLE (Francq and Zakoian, 2010) based on the likelihood in Eq. (10). Note that if Z_t is the residual of the ARMA process in Eq. (1) and (2), the MLE involves solving the sequential equations of all the ARMA(p,q) and GARCH($\tilde{p},\tilde{q}$) parameters.

2.2.2. Forecasting in GARCH($\tilde{p},\tilde{q}$)

The Eqs. (8) and (9) can be conveniently rewritten as the following (Andersen et al., 2003, Francq and Zakoian, 2010):

$$\begin{bmatrix} Z_t^2 \\ Z_{t-1}^2 \\ \vdots \\ Z_{t-r+1}^2 \\ \varepsilon_t \\ \varepsilon_{t-1} \\ \vdots \\ \varepsilon_{t-\tilde{p}+1} \end{bmatrix} = \begin{bmatrix} \omega \\ 0 \\ \vdots \\ 0 \\ 0 \\ 0 \\ \vdots \\ 0 \end{bmatrix} + \begin{bmatrix} \alpha_1+\beta_1 & \cdots & \alpha_r+\beta_r & -\beta_1 & \cdots & -\beta_{\tilde{p}} \\ 1 & & 0 & 0 & \cdots & 0 \\ \vdots & & & & & \\ 0 & \cdots & 1 & 0 & \cdots & 0 \\ 0 & \cdots & 0 & 0 & \cdots & 0 \\ 0 & \cdots & 0 & 1 & \cdots 0 & 0 \\ \vdots & & & & & \\ 0 & \cdots & 0 & 0 \cdots & 1 & 0 \end{bmatrix} \times \begin{bmatrix} Z_{t-1}^2 \\ Z_{t-2}^2 \\ \vdots \\ Z_{t-r}^2 \\ \varepsilon_{t-1} \\ \varepsilon_{t-2} \\ \vdots \\ \varepsilon_{t-\tilde{p}} \end{bmatrix} + \begin{bmatrix} \varepsilon_t \\ 0 \\ \vdots \\ 0 \\ \varepsilon_t \\ 0 \\ \vdots \\ 0 \end{bmatrix} \tag{11}$$

where $\varepsilon_t = Z_t^2 - \sigma_t^2 = (\eta_t^2 - 1)\sigma_t^2$, $\eta_t \sim N(0,1)$ and $r = \max(\tilde{p},\tilde{q})$.

In a matrix form, Eq. (11) is simplified:

$$\boldsymbol{\Xi}_t^2 = \omega\mathbf{e}_1 + \boldsymbol{\Gamma}\boldsymbol{\Xi}_{t-1}^2 + (\mathbf{e}_1 + \mathbf{e}_{m+1})\varepsilon_t \tag{12}$$

where $\mathbf{e}_i$ is a vector such that all the components are zero except the i^{th} component which is 1. $\boldsymbol{\Gamma}$ is the parameter matrix in the second term of the right side of Eq. (11) and $\boldsymbol{\Xi}_t^2$ is the vector in the left side of this equation.

Recursively, h-step ahead GARCH($\tilde{p},\tilde{q}$) process is expressed as:

$$\mathbf{\Xi}_{t+h}^{2} = \sum_{i=0}^{h-1}\mathbf{\Gamma}^{i}((\mathbf{e}_{1}+\mathbf{e}_{r+1})\varepsilon_{t+h-i}+\omega\mathbf{e}_{1})+\mathbf{\Gamma}^{h}\mathbf{\Xi}_{t}^{2} \tag{13}$$

The h-step ahead predictor for the conditional variance from the GARCH($\tilde{p},\tilde{q}$) process is:

$$E(Z_{t+h}^{2} \mid I_{t}) = E(\sigma_{t+h}^{2} \mid I_{t}) = \omega_{h} + \sum_{i=0}^{\tilde{p}-1}\delta_{i,h}\sigma_{t-i}^{2} + \sum_{i=0}^{r-1}\rho_{i,h}Z_{t-i}^{2} \tag{14}$$

where I_t is all the available information up to time t, and

$$\omega_{h} = \mathbf{e}_{1}'(\mathbf{1}+\mathbf{\Gamma}+\ldots+\mathbf{\Gamma}^{h-1})\mathbf{e}_{1}\omega$$

$$\delta_{i,h} = -\mathbf{e}_{1}'\mathbf{\Gamma}^{h}\mathbf{e}_{r+i+1} \qquad \text{for i=0,}\ldots, \tilde{p}\text{-1}$$

$$\rho_{i,h} = \begin{cases} \mathbf{e}_{1}'\mathbf{\Gamma}^{h}(\mathbf{e}_{i+1}+\mathbf{e}_{r+i+1}) & \text{for } i=0,\ldots, \tilde{p}-1 \\ \mathbf{e}_{1}'\mathbf{\Gamma}^{h}\mathbf{e}_{i+1} & \text{for } i=\tilde{p},\ldots, r-1 \end{cases} \tag{15}$$

where $\mathbf{1}$ is an identity matrix.

As an example, the predictor of the popular GARCH(1,1) process is illustrated:

$$E(\sigma_{t+h}^{2} \mid I_{t}) = \omega\sum_{i=0}^{h-1}(\alpha_{1}+\beta_{1})^{i} + (\alpha_{1}+\beta_{1})^{h-i}\alpha_{1}Z_{t}^{2} + (\alpha_{1}+\beta_{1})^{h-1}\beta_{1}\sigma_{t}^{2} \tag{16}$$

2.3. Dynamic Linear Models

2.3.1. State Space model and Dynamic Linear Models

State space models consider a time series as the output of a dynamic system perturbed by random disturbances (Künsch, 2001, Migon et al., 2005). Dynamic Linear Models (DLM) represent one of the important classes of state space models (West and Harrison, 1997, Petris et al., 2009). A DLM is specified for $\mathbf{X}_t$ with s variables ($s\times 1$) by a normal distribution for the m-dimensional **state vector** ($\mathbf{\Lambda}_t$). At time t=0,

$$\mathbf{\Lambda}_0 = N(\mathbf{m}_0, \mathbf{C}_0^{\Lambda}) \tag{17}$$

together with a pair of equations for each time $t \geq 1$,

$$\mathbf{X}_t = \mathbf{F}_t \mathbf{\Lambda}_t + \mathbf{V}_t \qquad \mathbf{V}_t \sim N(0, \mathbf{C}_t^V) \tag{18}$$

$$\mathbf{\Lambda}_t = \mathbf{G}_t \mathbf{\Lambda}_{t-1} + \mathbf{W}_t \qquad \mathbf{W}_t \sim N(0, \mathbf{C}_t^W) \tag{19}$$

where $\mathbf{F}_t$ and $\mathbf{G}_t$ are known $s \times m$ and $m \times m$ matrices; $\mathbf{V}_t$ and $\mathbf{W}_t$ are mutually independent error sequences with Gaussian (normal) distribution; $\mathbf{m}_0$ and $\mathbf{C}_0^{\Lambda}$ are the initial condition of the mean and covariance of the state vector $\mathbf{\Lambda}_t$; and $\mathbf{C}_t^V$ and $\mathbf{C}_t^W$ represent the time dependent covariance matrices. Note that Eq.(18) is the observation equation for the model defining the sampling distribution for $\mathbf{X}_t$ conditional on the quantity $\mathbf{\Lambda}_t$ while Eq.(19) is the evolution, state or system equation, defining the time evolution of the state vector.

If the matrices $\mathbf{F}_t$ and $\mathbf{G}_t$ are constant for all values of *t*, then the model is referred to as a time series DLM (TSDLM) and if the covariance matrices $\mathbf{C}_t^V$ and $\mathbf{C}_t^W$ are constant for all time *t*, then the model is referred as a constant DLM (CDLM). In the current study, we use the constant time series DLM (**TCDLM**) such that $\mathbf{F}_t = \mathbf{F}$, $\mathbf{G}_t = \mathbf{G}$, $\mathbf{C}_t^V = \mathbf{C}^V$ and $\mathbf{C}_t^W = \mathbf{C}^W$.

The ARMA model in Eq.(1) is also represented by the TCDLM model as:

$$X_t = \mathbf{F}\Lambda_t \tag{20}$$

$$\Lambda_t = \mathbf{G}\Lambda_{t-1} + \Theta Z_t \tag{21}$$

where

$$\mathbf{F} = [1 \quad 0 \Lambda \; 0] \tag{22}$$

$$\Theta = [1 \;\; \theta_1 \;\; \ldots \theta_{r-1}]' \tag{23}$$

and

$$\mathbf{G} = \begin{bmatrix} \phi_1 & 1 & 0 & \ldots 0 \\ \phi_2 & 0 & 1 & \ldots 0 \\ \vdots & \vdots & \vdots & \ldots 0 \\ \phi_{r-1} & 0 & 0 & \ldots 1 \\ \phi_r & 0 & 0 & \ldots 0 \end{bmatrix} \tag{24}$$

and $r = \max\{p, q+1\}$, $\phi_j = 0$ for $j>p$ and $\theta_j = 0$ for $j>q$.

Furthermore, the k^{th} order polynomial trend model (Godolphin and Harrison, 1975, Abraham and Ledolter, 1983), denoted as Trend(k+1), for a univariate time series is described with the DLM also as:

$$\mathbf{F} = [1 \quad 0 \quad \cdots \quad 0] \tag{25}$$

$$\mathbf{G} = \begin{bmatrix} 1 & 1 & 0 & \ldots & 0 \\ 0 & 1 & 1 & \ldots & 0 \\ \vdots & \vdots & \vdots & \ldots & \\ 0 & 0 & \ldots & 1 & 1 \\ 0 & 0 & 0 & \ldots 0 & 1 \end{bmatrix} \tag{26}$$

and

$$\mathbf{C}^W = diag(\sigma^2_{W_1}, \ldots, \sigma^2_{W_k}) \text{ and } \mathbf{C}^V = \sigma^2_V \tag{27}$$

The random walk plus noise model or local level model (Petris et al., 2009) is the special case of the polynomial trend model (Trend(1)) defined by:

$$X_t = \mu_t + V_t \qquad V_t \sim N(0, \sigma^2_V) \tag{28}$$

$$\mu_t = \mu_{t-1} + W_t \qquad W_t \sim N(0, \sigma^2_W) \tag{29}$$

where s=m=1 and F=G=1. Also, the linear trend model, Trend(2) is presented from Eqs. (25), (26), and (27) as:

$$\mathbf{F} = [1 \quad 0] \tag{30}$$

$$\mathbf{G} = \begin{bmatrix} 1 & 1 \\ 0 & 1 \end{bmatrix} \tag{31}$$

and $\mathbf{C}^V = \sigma_V^2$ and $\mathbf{C}^W = diag(\sigma_{W_1}^2, \sigma_{W_2}^2)$.

The ARMA model and the polynomial trend model can be combined through the TCDLM representation, and will be denoted as Trend(k+1)-ARMA(p,q). For example, the combination of the Trend (2)-ARMA(2,0) model is:

$$\mathbf{F} = [1 \;\; 0 \;\; 1 \;\; 0] \tag{32}$$

$$\mathbf{G} = \begin{bmatrix} 1 & 1 & 0 & 0 \\ 0 & 1 & 0 & 0 \\ 0 & 0 & \phi_1 & 0 \\ 0 & 0 & \phi_2 & 0 \end{bmatrix} \tag{33}$$

and $\mathbf{C}^V = \sigma_V^2$ and $\mathbf{C}^W = diag(\sigma_{W_1}^2, \sigma_{W_2}^2, \sigma_Z^2, 0)$.

2.3.2. Kalman filter for parameter estimation and forecasting

Since all the related distributions are normal, they are completely determined by the first and second moments (i.e. mean and variance). The Kalman filter (Kalman, 1960) gives us the solution for the intricate problem of parameter estimation and forecasting for DLM. The Kalman filter (Snyder, 1985) is an algorithm for efficiently doing exact inference in a linear dynamic system. Three propositions for Kalman filter, smoothing, and forecasting are described in the following. The first and second propositions (Kalman filtering and smoothing) are employed in the parameter estimation while the third proposition (Kalman forecasting) is used for forecasting.

Proposition 1 (Kalman filtering): Consider the DLM in Eqs. (18) and (19), starting from Eq.(17) let

$$\mathbf{\Lambda}_{t-1} \mid \mathbf{x}_{1:t-1} = N(\mathbf{m}_{t-1}, \mathbf{C}_t^{\Lambda}) \tag{34}$$

where $\mathbf{x}_{1:t-1}$ presents the observed $\mathbf{X}$ data for the time periods from 1 to *t*-1.

Then,

(i) The one-step-ahead predictive distribution of $\mathbf{\Lambda}_t$ given $\mathbf{x}_{1:t-1}$ is normal with parameters:

$$\mathbf{a}_t = E(\mathbf{\Lambda}_t \mid \mathbf{x}_{1:t-1}) = \mathbf{G}_t \mathbf{m}_{t-1} \tag{35}$$

$$\mathbf{R}_t = Var(\mathbf{\Lambda}_t \mid \mathbf{x}_{1:t-1}) = \mathbf{G}_t \mathbf{C}_{t-1}^{\Lambda} \mathbf{G}_t' + \mathbf{C}_t^{W} \tag{36}$$

(ii) The one-step-ahead predictive distribution of $\mathbf{X}_t$ given $\mathbf{x}_{1:t-1}$ is normal with parameters:

$$\mathbf{f}_t = E(\mathbf{X}_t \mid \mathbf{x}_{1:t-1}) = \mathbf{F}_t \mathbf{a}_t \tag{37}$$

$$\mathbf{Q}_t = Var(\mathbf{X}_t \mid \mathbf{x}_{1:t-1}) = \mathbf{F}_t \mathbf{R}_t \mathbf{F}_t' + \mathbf{C}_t^{V} \tag{38}$$

(iii) The filtering distribution of $\mathbf{\Lambda}_t$ given $\mathbf{x}_{1:t}$ is normal with parameters:

$$\mathbf{m}_t = E(\mathbf{\Lambda}_t \mid \mathbf{x}_{1:t}) = \mathbf{a}_t + \mathbf{R}_t \mathbf{F}_t' \mathbf{Q}_t^{-1} (\mathbf{X}_t - \mathbf{f}_t) \tag{39}$$

$$\mathbf{C}_t^{\Lambda} = Var(\mathbf{\Lambda}_t \mid \mathbf{x}_{1:t}) = \mathbf{R}_t - \mathbf{R}_t \mathbf{F}_t' \mathbf{Q}_t^{-1} \mathbf{F}_t \mathbf{R}_t \tag{40}$$

In time series analysis it is often the case that one wants to reconstruct the behavior of the system (i.e. backward estimation of all the observed states). This is called the smoothing recursion which can be stated in terms of means and variances as follows. Suppose that the observations are available up to the time period *n* as $\mathbf{x}_{1:n}$, then:

Proposition 2 (Kalman smoother)

If $\mathbf{\Lambda}_{t+1} \mid \mathbf{x}_{1:n} \sim N(\mathbf{s}_{t+1}, \mathbf{C}_{t+1}^{S})$, then

$$\mathbf{\Lambda}_t \mid \mathbf{x}_{1:n} \sim N(\mathbf{s}_t, \mathbf{C}_t^{S}) \tag{41}$$

where

$$\mathbf{s}_t = E(\mathbf{\Lambda}_t \mid \mathbf{x}_{1:n}) = \mathbf{m}_t + \mathbf{C}_t^{\Lambda} \mathbf{G}_{t+1}' \mathbf{R}_{t+1}^{-1} (\mathbf{s}_{t+1} - \mathbf{a}_{t+1}) \tag{42}$$

$$\mathbf{C}_t^S = Var(\mathbf{\Lambda}_t \mid \mathbf{x}_{1:n}) = \mathbf{C}_t^\Lambda - \mathbf{C}_t^\Lambda \mathbf{G}_{t+1}' \mathbf{R}_{t+1}^{-1} (\mathbf{R}_{t+1} - \mathbf{C}_{t+1}^S) \mathbf{R}_{t+1}^{-1} \mathbf{G}_{t+1} \mathbf{C}_t^\Lambda \tag{43}$$

As for the filtering and smoothing described in Propositions 1 and 2, the forecasting distribution can be explicitly described for the lead time $h \geq 1$ because of the normality assumption as:

Proposition 3 (Kalman forecasting)

(i) The distribution of $\mathbf{\Lambda}_{t+h}$ given $\mathbf{x}_{1:t}$ is normal with parameters:

$$\mathbf{a}_t(h) = E(\mathbf{\Lambda}_{t+h} \mid \mathbf{x}_{1:t}) = \mathbf{G}_{t+h} \mathbf{a}_t(h-1) \tag{44}$$

$$\mathbf{R}_t(h) = Var(\mathbf{\Lambda}_{t+h} \mid \mathbf{x}_{1:t}) = \mathbf{G}_{t+h} \mathbf{R}_t(h-1) \mathbf{G}_{t+h}' + \mathbf{C}_{t+h}^W \tag{45}$$

where $\mathbf{a}_t(0) = \mathbf{m}_t$ and $\mathbf{R}_t(0) = \mathbf{C}_t^\Lambda$

(ii) The distribution of $\mathbf{X}_t$ given $\mathbf{x}_{1:t-1}$ is normal with parameters:

$$\mathbf{f}_t(h) = E(\mathbf{X}_{t+h} \mid \mathbf{x}_{1:t}) = \mathbf{F}_{t+h} \mathbf{a}_t(h) \tag{46}$$

$$\mathbf{Q}_t(h) = Var(\mathbf{X}_{t+h} \mid \mathbf{x}_{1:t}) = \mathbf{F}_{t+h} \mathbf{R}_t(h) \mathbf{F}_{t+h}' + \mathbf{C}_t^V \tag{47}$$

Note that in TCDLM, the propostions 1-3 are much simplified by $\mathbf{F}_t = \mathbf{F}$, $\mathbf{G}_t = \mathbf{G}$, $\mathbf{C}_t^V = \mathbf{C}^V$ and $\mathbf{C}_t^W = \mathbf{C}^W$ for all t.

To estimate the parameters of the DLMs, MLE is applied maximizing the likelihood defined as:

$$L(\boldsymbol{\psi}) = -\frac{1}{2} \sum_{t=1}^{n} \log \left| \mathbf{Q}_t \right| - \frac{1}{2} \sum_{t=1}^{n} (\mathbf{X}_t - \mathbf{f}_t)' \mathbf{Q}_t^{-1} (\mathbf{X}_t - \mathbf{f}_t) \tag{48}$$

where, $\boldsymbol{\psi}$ represents all the parameters in Eqs. (18) and (19). The optimization problem in Eq. (48) is solved through the Limited memory Broyden–Fletcher–Goldfarb–Shanno method for Bound-constrained optimization (L-BFGS-B) method (Petris et al., 2009). This is the only method accepting restrictions in parameter spaces. Furthermore, the Bayesian parameter estimation procedure for DLMs has been established assuming the prior distributions of the parameters (Petris et al., 2009, West and Harrison, 1997).

2.4. EMD and NSOR

Lee and Ouarda (2012) proposed a stochastic simulation model to adequately reproduce the smoothly varying nonstationary oscillation (NSO) processes embedded in observed data. The proposed model employed a cutting-edge decomposition technique (Huang et al., 1998, Huang and Wu, 2008), called Empirical Mode Decomposition (EMD). Also nonparametric time series models, k-nearest neighbor resampling (Lall and Sharma, 1996) and block bootstrapping, are employed. This is called NSO resampling (NSOR). The overall procedure of the EMD-NSOR prediction is:

(1) Decompose the concerned time series (X_t) into a finite number of IMFs.

(2) Select significant IMF components using the significance test (Wu and Huang, 2004) and subjective criteria (Lee and Ouarda, 2010b).

(3) Fit stochastic time series models according to the nature of the components determined in step (2). In the current study, significant IMF components are modeled using NSOR (discussed later) and the residuals are modeled using order-1 autoregressive (AR(1)).

(4) Predict the IMF components using the fitted models (NSOR and AR(1)).

(5) Sum up the forecasted IMFs from each mode.

A brief summary of the NSOR for the selected IMF component(s) is:

(1) A block length, L_B, is randomly generated from a discrete distribution (e.g., Geometric or Poisson). A Poisson distribution is employed in the current study as in Lee and Ouarda (2010a). More information on the selection of this discrete distribution in block bootstrapping can be found in Lee (2008). The related parameter is selected using variance inflation factor (VIF) (Lee and Ouarda, 2012, Wilks, 1997) .

(2) The weighted distances between the current and observed values as well as the change rates of the current and the observed values are estimated for each observed value. The variances in the change rate and the original sequences are employed as weights. Here the change rate is defined as the difference between the current value and the immediate preceding value of an IMF component.

(3) The time indices of the k-smallest distances among the observed record length, where k is the tuning parameter, are estimated by $k = \sqrt{N}$ as a heuristic approach (Lall and Sharma, 1996, Lee and Ouarda, 2011a).

(4) One of the k time indices is selected with the weighted probability of the inverse of the order index (i.e., $1/j$, j=1, 2,…, k) with unity scaling.

(5) The following L_B change rate values in the subsequent time of the selected index are taken and subsequently combined with the previous state to comprise the real domain values.

3. Data Description

For the current study, the climate indices ENSO and PDO are selected as it is known to be teleconnected with the hydro-climatological variables of the Great Lakes system (Lee and Ouarda, 2010c). A brief description of each of these climate indices is provided in the following paragraphs.

The ENSO is a climatic pattern occurring across the tropical Pacific Ocean, causing climate variability on 3~7 year periods (Alexander et al., 2002). Among various ENSO indices (Trenberth, 1997), the multivariate ENSO index developed by Wolter and Timlin (1993) is employed in the current study since this is the only index that includes at least the fundamental tropical atmospheric bridges. The dataset, ranging from 1950-2009 was downloaded from http://www.esrl.noaa.gov/psd/people/klaus.wolter/MEI/.

The PDO index represents the leading principal component of sea-surface temperature anomalies in the North Pacific Ocean, polewards of 20^{o}N. Among a number of PDO indices, the most commonly used one, developed by Mantua and Zhang and their colleagues (Mantua et al., 1997, Zhang et al., 1997), was employed in the current study with the dataset ranging from 1900-2009. It was downloaded from http://jisao.washington.edu/pdo/PDO.latest.

4. Forecasting Monthly ENSO

4.1. Preliminary analysis and application methodology for monthly ENSO index

The annual and monthly time series of the employed ENSO index are presented in Figure 1(a) and (b). The monthly time series presents strong persistency as shown in Figure 1(c) while the annual time series shows weak serial dependence (only 0.285 for lag-1 autocorrelation function (ACF) during the period 1950-2009. Figure 2 indicates that the monthly statistics of the ENSO index does not show evident seasonal variations. The spectral density of the monthly ENSO index shown in Figure 1(d) illustrates this. The scatter plots in Figure 3 reveal the linear relations for different lead times of monthly ENSO indices. Note from this figure that the association in low values is higher than in high values through all different lead times. In turn, one can suspect the existence of heteroscedasticity (differing variance). Therefore, we also applied the GARCH model to this index. Furthermore, different orders of ARMA(p,q) models have been tested as well as the DLM and EMD-NSOR.

Among others, the results of the following models are presented:

(1) ARMA(1,0)

(2) ARMA(4,0)

(3) ARMA(7,3)

(4) ARMA(8,5)

(5) DLM: Trend (1)-ARMA(4,0)

(6) ARMA(4,0) – GARCH(1,1)

The selection of the order of the ARMA models was based on the AIC in Eq. (5). The AIC values corresponding to the various ARMA(p,q) models with p=0,…,10 and q=0,…,10 are presented in Table 1. Even though ARMA(8,5) presents the smallest AIC, other low order models with relatively small AIC values are also selected, such as ARMA(4,0) and ARMA(1,0) for comparison purposes. Note that ARMA(4,0) has the second smallest AIC value in Table 1. In DLM and GARCH models, the ARMA model should be selected as a base model. A low order ARMA model is preferred due to parsimony issues. Therefore, ARMA(4,0) is selected for the combination in DLM and GARCH models. We also tested other ARMA models with different models but the results showed no improvement over ARMA(4,0).

4.2. Results

To validate the model performance, the first 40 years of record of the monthly ENSO index (1950-1989) were employed to fit the models. Then, the last 20 year of record (1990-2009) were forecasted for each month. Depending on the selected model, different numbers of predictors were used to make predictions for succeeding months. For example, for the ARMA(4,0) model, four preceding months were used as predictors. Consequently, in order to make predictions for January-December 1990 (i.e. h=1,…, 12 where h is the lead time), four months from September-December 1989 were used. For further details, the reader is referred to section 2.

The correlation and root mean square error (RMSE) between the forecasted values and the observations were estimated. Note that higher correlations and lower RMSE values represent models with better performances. These results are presented in Table 2 and Table 3 as well as Figure 4.

Figure 4(a) presents a comparison of the RMSE of the ARMA(p,q) models. The figure indicates that the higher order ARMA models (i.e. ARMA(7,3) and ARMA(8,5)) do not show significantly better performances than ARMA(4,0). The RMSE of the ARMA(4,0) model is also significantly lower than ARMA(1,0) for all lead times (h). Figure 4(b) shows that a substantial improvement in performance is obtained with Trend(1)-ARMA(4,0) and ARMA(4,0)-GARCH(1,1) models in comparison to ARMA(4,0). On the other hand, no significant difference is observed between the two models Trend(1)-ARMA(4,0) and ARMA(4,0)-GARCH(1,1). EMD-NSOR presents the worst performance among all models. This result may be intuitive as the EMD-NSOR model was developed mainly to characterize the long-term oscillation pattern in a series (Lee and Ouarda, 2010b), and hence does not lead to good performances for short-term forecasting.

The correlations between the forecasted values and the observations illustrate similar results to the RMSE as illustrated in Table 3, Figure 4(c) and (d). In Figure 4(c), it is observed that no significant performance improvement with higher order ARMA models (i.e. ARMA(7,3) and ARMA(8,5)) is detected except that for long lead times (h>9) these higher order models present a slightly better performance. Figure 4(d) presents somewhat different results from the RMSE in Figure 4(b). Trend(1)-ARMA(4,0) shows a better performance over the shorter lead times (h=2-7 month) and worse than ARMA(4,0) during the longer lead times (h=9-12 month). The ARMA(4,0)-GARCH(1,1) model presents consistently better results overall lead times. Recall that the monthly ENSO index presents the heteroscedasticity over all different lead times shown in the scatter plots of Figure 3. It is well documented that GARCH can reproduce the heteroscedasticity characteristics (Engle, 2002).

The forecasting results corresponding to 1- 6 month lead times are presented for ARMA(4,0), ARMA(7,3), Trend(1)-ARMA(4,0), and ARMA(4,0)-GARCH(1,1) in Figure 5, Figure 6, Figure 7, and Figure 8, respectively. As the prediction lead time (h) increases, the 95 percent upper and lower limits get wider. The maximum observation and its neighbors in year 1997-1998 are less predictable as h increases for all the tested models.

5. Forecasting Monthly PDO

5.1. Preliminary analysis and application methodology for monthly PDO index

The annual and monthly time series of the employed PDO index are presented in Figure 9(a) and (b), respectively. The monthly time series presents strong persistency as shown in Figure 9(b) while the annual time series also shows significant serial dependency (0.5245 of lag-1 ACF in Figure 9(c) during the period (1900-2009). Figure 10 indicates that the monthly statistics of the ENSO index do not show much seasonal variation. The scatter plots in Figure 11 reveal linear relations for all lead times for the monthly PDO index. Variation difference along the values (i.e. heteroscedasticity) is not observed. Different orders of ARMA(p,q) models as well as both DLM models have been tested.

Among others, the results of the following models are presented:

(1) ARMA(1,0)

(2) ARMA(5,0)

(3) ARMA(9,7)

(4) ARMA(28,0)

(5) DLM-Trend 1 and ARMA(1,0)

(6) DLM-Trend 2 and ARMA(2,0)

The selection of the order of ARMA models was based on the AIC in Eq. (5) for p=0,…,10 and q=1,…,10 (result not shown). The AIC shows that ARMA(9,7) is the best order selection. Similar findings for the same data to this order selection was reported by Nairn-Birch et al. (2009) whose study was for the simulation of this index. The relatively low-order model ARMA(5,0) and high-order model ARMA(28,0) as well as both DLM models were also tested. Note that ARMA(28,0) is the best order among p orders without moving average term (i.e. q=0).

5.2. Results

To validate the model performance, the first 90 years of the monthly PDO index (1900-1989) were employed to fit the models. The last 20 year records (1990-2009) were forecasted at each month for h=1,…,12. The correlation and root mean square error (RMSE) between the forecasted values and the observations were estimated as presented in Table 4 and Table 5, respectively. These results are also graphically illustrated in Figure 12.

In Table 4 and the top panel of Figure 12, the RMSE of the tested models are compared. The figure indicates that the higher order ARMA models (i.e. ARMA(9,7) and ARMA(28,0)) show significantly better performances than lower order ARMA models (i.e. ARMA(1,0) and ARMA(5,0)) while the RMSE of ARMA(28,0) is much lower than ARMA(9,7) for all lead times (h). The two DLM models present much worse performances than the selected ARMA models for forecasting the PDO index over all the lead times. We also tested higher order ARMA models with the trend component for DLM but no improved results were obtained.

In Table 5 and the bottom panel of Figure 12, it can be observed that the results of the correlations between the forecasted values and the observations show much different behavior from the RMSE results. While the ARMA(28,0) model still performs best for short lead times ($h<8$), the ARMA(9,7) model shows the worst performance among the selected models. For long lead times ($h>8$), the low-order ARMA models (ARMA(1,0) and ARMA(5,0)) show the best performances.

The forecasting results corresponding to 1-6 month lead times are presented for ARMA(9,7) and ARMA(28,0) in Figure 13 and Figure 14, respectively. As the prediction lead time (h) increases, the 95 percent upper and lower limits get wider. The 6-month lead time shows excessively wide upper and lower limits. The wide range of the limits and the behavior of the bottom panel of Figure 12 described above imply that forecasting longer than 6 month lead times is not skillful regardless of the selected model.

We also tested the EMD-NSOR model. Even though the prediction was successful in some cases as shown in Figure 15, the overall prediction skill was no better than even low-order ARMA models (see Table 6). Also, the ARMA-GARCH model was also tested and the results showed a prediction skill than is not better than the sole ARMA model as shown in Table 6.

6. Summary and Conclusions

It is commonly known that climate indices are good representatives of the current climate system and thus good predictors for hydro-meteorological variables, specifically for the NBS components of the Great Lakes. In the current study, we forecasted the monthly climate index (ENSO) up to 12 month lead time using a number of time series models including the traditional ARMA model and the DLM, GARCH, and EMD-NSOR models.

For the ENSO index, results indicated that the ARMA(4,0)-GARCH(1,1) model is superior to the other tested models in forecasting the monthly ENSO index and the DLM model (Trend(1)-ARMA(4,0)) shows the lowest RMSE while the correlation performance measurement revealed that Trend(1)-ARMA(4,0) does not perform as well for long lead times (i.e. h>8). The reason for the better representation by the GARCH process is the presence of heteroscedasticity in the ENSO index.

For the PDO index, results showed that the typical ARMA models are superior to the other tested models with the agreement between the observed and forecasted values. The forecasted values for longer than 6-month lead times from all the selected models illustrate wide confidence intervals. This implies that the forecasting is not much meaningful for the longer than 6-month lead times. The long-term oscillation model, EMD-NSOR, presents no useful skill for the short-term forecasting of the climate indices.

The forecasted climate indices can be employed as predictors for the NBS components of the Great Lakes system in future studies.

Acknowledgment

Note that the current manuscript has been produced by the International Joint Commission (IJC) for the management of the great lakes. The manuscript has never submitted it for publication in a journal.

Funding: This work was supported by the National Research Foundation of Korea (NRF) grant funded by the Korean Government (MEST) (2018R1A2B6001799).

Author contribution: TS carried out selecting methods and programed the models used as well as drafted the manuscript. TO supervised the study and edited the manuscript.

Code Availability: Code is available upon request to the corresponding author.

Availability of data: The climate indices data used in the current study is already available to public. The website is mentioned in the manuscript.

Compliance with ethical standards

Conflict of interest: The authors declare that no competing interests.

Notations:

t : time index

X_t : time dependent variable

$\mathbf{X}_t$: vector of multivariate time dependent variables

Z_t : time independent white noise variable or its square is time dependent in the representation of GARCH model

p, q : mode order of ARMA model

θ, ϕ : parameters of ARMA model

n , n_{par} : number of observations and parameters, respectively

h : prediction lead time

$\hat{X}_n(h)$: h-step ahead forecast, X_{n+h}

$L(.)$: likelihood

B : backward shift operator

μ, σ^2 : mean and variance

$\mathbf{C}$: covariance matrix

$\boldsymbol{\psi}$:parameter set of a model

α, β :parameters of GARCH model

$\boldsymbol{\Lambda}_t$:m-dimensional state vector

$\mathbf{V}_t, \mathbf{W}_t$:mutually independent error sequences with normal distribution

$\mathbf{F}_t, \mathbf{G}_t$: parameter and evolution matrices in DLM

References

Abraham, B. and Ledolter, J. (1983) *Statistical methods for forecasting*.

Ahn, J. H. and Kim, H. S. (2005), Nonlinear modeling of El Nino/southern oscillation index, *Journal of Hydrologic Engineering*, **10,** 8-15.

Alexander, M. A., Blade, I., Newman, M., Lanzante, J. R., Lau, N. C. and Scott, J. D. (2002), The atmospheric bridge: The influence of ENSO teleconnections on air-sea interaction over the global oceans, *Journal of Climate*, **15,** 2205-2231.

Andersen, T. G., Bollerslev, T., Diebold, F. X. and Labys, P. (2003), Modeling and forecasting realized volatility, *Econometrica*, **71,** 579-625.

Bollerslev, T. (1986), Generalized autoregressive conditional heteroskedasticity, *Journal of Econometrics*, **31,** 307-327.

Bollerslev, T., Chou, R. Y. and Kroner, K. F. (1992), ARCH modeling in finance. A review of the theory and empirical evidence, *Journal of Econometrics*, **52,** 5-59.

Bosley, T. M., Alorainy, I. A., Salih, M. A., Aldhalaan, H. M., Abu-Amero, K. K., Oystreck, D. T., Tischfield, M. A., Engle, E. C. and Erickson, R. P. (2008), The clinical spectrum of homozygous HOXA1 mutations, *American Journal of Medical Genetics Part A*, **146A,** 1235-1240.

Brockwell, P. J. and Davis, R. (1988), Simple consistent estimation of the coeffcients of a linear filter, *Stochastic Process Application*, **28,** 47-59.

Brockwell, P. J. and Davis, R. A. (2003) *Introduction to Time Series and Forecasting*, Springer, Harrisonburg, VA.

Burg, J. (1978) *A new analysis technique for time series data*, John Wiley & Sons Inc, New York. .

Chen, D., Cane, M. A., Kaplan, A., Zebiak, S. E. and Huang, D. J. (2004), Predictability of El Nino over the past 148 years, *Nature*, **428,** 733-736.

Cheng, Y. J., Tang, Y. M., Jackson, P., Chen, D. K., Zhou, X. B. and Deng, Z. W. (2010a), Further analysis of singular vector and ENSO predictability in the Lamont model-Part II: singular value and predictability, *Climate Dynamics,* **35,** 827-840.

Cheng, Y. J., Tang, Y. M., Zhou, X. B., Jackson, P. and Chen, D. K. (2010b), Further analysis of singular vector and ENSO predictability in the Lamont model-Part I: singular vector and the control factors, *Climate Dynamics,* **35,** 807-826.

Elek, P. and Márkus, L. (2004), A long range dependent model with nonlinear innovations for simulating daily river flows, *Natural Hazards and Earth System Science,* **4,** 277-283.

Engle, R. (2001), GARCH 101: The use of ARCH/GARCH models in applied econometrics, *Journal of Economic Perspectives,* **15,** 157-168.

Engle, R. (2002), New frontiers for arch models, *Journal of Applied Econometrics,* **17,** 425-446.

Engle, R. F. (1982), Autoregressive Conditional Heteroscedasticity with Estimates of the Variance of United Kingdom Inflation, *Econometrica*, **50,** 987-1007.

Engle, R. F. and Kroner, K. F. (1995), Multivariate Simultaneous Generalized Arch, *Econometric Theory,* **11,** 122-150.

Fan, J. and Yao, Q. (2003) *Nonlinear Time Series - Nonparametric and Parametric Methods,* Springer, New York.

Francq, C. and Zakoian, J.-M. (2010) *GARCH Models: Structure, Statistical Inference and Financial Applications*, Chippenham, United Kingdom.

Godolphin, E. and Harrison, P. (1975), Equivalence theorems for polynomial projecting predictors. , *Journal of the Royal Statistical Society Series B-Stat Methodology,* **B 35,** 205 – 215.

Hannan, E. J. and Rissanen, J. (1982), Recursive estimation of mixed autoregressive-moving average order, *Biometrika* **69,** 81-94.

Huang, N. E., Shen, Z., Long, S. R., Wu, M. L. C., Shih, H. H., Zheng, Q. N., Yen, N. C., Tung, C. C. and Liu, H. H. (1998), The empirical mode decomposition and the Hilbert spectrum for nonlinear and non-stationary time series analysis, *Proceedings of the Royal Society of London Series a-Mathematical Physical and Engineering Sciences,* **454,** 903-995.

Huang, N. E. and Wu, Z. H. (2008), A review on Hilbert-Huang transform: method and its applications to geophysical studies, *Reviews of Geophysics,* **46,** RG2006.

Immerzeel, W. W. and Bierkens, M. F. P. (2010), Seasonal prediction of monsoon rainfall in three Asian river basins: the importance of snow cover on the Tibetan Plateau, *International Journal of Climatology,* **30,** 1835-1842.

Künsch, H. R. (2001) *State space and hidden Markov models In Complex Stochastic Systems* Chapman and Hall/CRC, Boca Raton, FL.

Kalman, R. E. (1960), A New Approach to Linear Filtering and Prediction Problems, *Transactions of the ASME-Journal of Basic Engineering,* **82,** 35-45.

Kirtman, B. P. and Min, D. (2009), Multimodel ensemble ENSO prediction with CCSM and CFS, *Monthly Weather Review,* **137,** 2908-2930.

Lall, U. and Sharma, A. (1996), A nearest neighbor bootstrap for resampling hydrologic time series, *Water Resources Research,* **32,** 679-693.

Lee, T. and Ouarda, T. B. M. J. (2010a), Long-term prediction of precipitation and hydrologic extremes with nonstationary oscillation processes, *Journal of Geophysical Research Atmospheres,* **115,** D13107.

Lee, T. and Ouarda, T. B. M. J. (2010b), Long-term prediction of precipitation and hydrologic extremes with nonstationary oscillation processes, *Journal of Geophysical Research-Atmospheres,* **115,** doi:10.1029/2009JD012801.

Lee, T. and Ouarda, T. B. M. J. (2010c) INRS-ETE, Quebec, pp. 78.

Lee, T. and Ouarda, T. B. M. J. (2011a), Identification of model order and number of neighbors for k-nearest neighbor resampling, *Journal of Hydrology*, **404,** 136-145.

Lee, T. and Ouarda, T. B. M. J. (2011b), Prediction of climate nonstationary oscillation processes with empirical mode decomposition, *Journal of Geophysical Research Atmospheres*, **116**.

Lee, T. and Ouarda, T. B. M. J. (2012), Stochastic simulation of nonstationary oscillation hydroclimatic processes using empirical mode decomposition, *Water Resources Research*, **48**.

Lee, T. S. (2008) In *Civil and Environmental Engineering*, Vol. Ph. D. Colorado State University, Fort Collins, CO., USA, pp. 346.

Mantua, N. J., Hare, S. R., Zhang, Y., Wallace, J. M. and Francis, R. C. (1997), A Pacific interdecadal climate oscillation with impacts on salmon production, *Bulletin of the American Meteorological Society*, **78,** 1069-1079.

Migon, H., Gamerman, D., Lopez, H. and Ferreira, M. (2005) In *Handbook of Statistics*(Eds, Day, D. and Rao, C.) Elsevier, New York, pp. 553-588.

Modarres, R. and Ouarda, T. B. M. J. (2013a), Generalized autoregressive conditional heteroscedasticity modelling of hydrologic time series, *Hydrological Processes*, **27,** 3174-3191.

Modarres, R. and Ouarda, T. B. M. J. (2013b), Modeling rainfall-runoff relationship using multivariate GARCH model, *Journal of Hydrology*, **499,** 1-18.

Modarres, R. and Ouarda, T. B. M. J. (2014), A generalized conditional heteroscedastic model for temperature downscaling, *Climate Dynamics*, **43,** 2629-2649.

Nairn-Birch, N., Diez, D., Eslami, E., Fauria, M. M., Johnson, E. A. and Schoenberg, F. P. (2009), Simulation and estimation of probabilities of phases of the Pacific Decadal Oscillation, *Environmetrics,* **22,** 79–85.

Naizghi, M. S. and Ouarda, T. B. M. J. (2017), Teleconnections and analysis of long-term wind speed variability in the UAE, *International Journal of Climatology,* **37,** 230-248.

Niranjan Kumar, K., Ouarda, T. B. M. J., Sandeep, S. and Ajayamohan, R. S. (2016), Wintertime precipitation variability over the Arabian Peninsula and its relationship with ENSO in the CAM4 simulations, *Climate Dynamics,* **47,** 2443-2454.

Ouachani, R., Bargaoui, Z. and Ouarda, T. (2013), Power of teleconnection patterns on precipitation and streamflow variability of upper Medjerda Basin, *International Journal of Climatology,* **33,** 58-76.

Petris, G., Petrone, S. and Campagnoli, P. (2009) *Dynamic Linear Models with R*, Springer, New York.

Rodionov, S. and Assel, R. A. (2003), Winter severity in the Great Lakes region: a tale of two oscillations, *Climate Research,* **24,** 19-31.

Salas, J. D., Delleur, J. W., Yevjevich, V. and Lane, W. L. (1980) *Applied Modeling of Hydrologic Time Series*, Water Resources Publications, Littleton, Colorado.

Schneider, E. K., Huang, B., Zhu, Z., Dewitt, D. G., Kinter Iii, J. L., Kirtman, B. P. and Shukla, J. (1999), Ocean data assimilation, initialization, and predictions of ENSO with a coupled GCM, *Monthly Weather Review,* **127,** 1187-1207.

Snyder, R. D. (1985), Recursive Estimation of Dynamic Linear Models, *Journal of the Royal Statistical Society. Series B (Methodological),* **47,** 272-276.

Thomas, B. E. (2007), Climatic fluctuations and forecasting of streamflow in the lower Colorado River Basin, *Journal of the American Water Resources Association,* **43,** 1550-1569.

Trenberth, K. E. (1997), The definition of El Nino, *Bulletin of the American Meteorological Society*, **78,** 2771-2777.

Tsonis, A. A., Elsner, J. B. and Sun, D.-Z. (2007) In *Nonlinear Dynamics in Geosciences*Springer New York, pp. 537-555.

Walker, G. T. (1932), On periodicity in series of related terms, *Proceedings of the Royal Society A*, **131** 518-532.

Wang, W., Van Gelder, P. H. A. J. M., Vrijling, J. K. and Ma, J. (2005), Testing and modelling autoregressive conditional heteroskedasticity of streamflow processes, *Nonlinear Processes in Geophysics,* **12,** 55-66.

West, M. and Harrison, J. (1997) *Bayesian Forecasting and Dynamic Models*, Springer, New York.

Westra, S. and Sharma, A. (2010), An Upper Limit to Seasonal Rainfall Predictability?, *Journal of Climate,* **23,** 3332-3351.

Wilks, D. S. (1997), Resampling Hypothesis Tests for Autocorrelated Fields, *Journal of Climate,* **10,** 65-82.

Wolter, K. and Timlin, M. S. (1993) In *Proc. of the 17th Climate Diagnostics Workshop*NOAA/NMC/CAC, NSSL, Oklahoma Clim. Survey, CIMMS and the School of Meteor., Univ. of Oklahoma, Norman, OK, pp. 52-57.

Wu, R. and Kirtman, B. P. (2003), On the impacts of the Indian summer monsoon on ENSO in a coupled GCM, *Quarterly Journal of the Royal Meteorological Society,* **129,** 3439-3468.

Wu, Z. H. and Huang, N. E. (2004), A study of the characteristics of white noise using the empirical mode decomposition method, *Proceedings of the Royal Society of London Series a-Mathematical Physical and Engineering Sciences,* **460,** 1597-1611.

Yule, G. U. (1927), On a method of investigating periodicities in disturbed series, with special reference to Wolfer's sunspot numbers, *Philosophical Transactions of the Royal Society London Series A,* **226** 267-298.

Zhang, Y., Wallace, J. M. and Battisti, D. S. (1997), ENSO-like interdecadal variability: 1900-93, *Journal of Climate,* **10,** 1004-1020.

Table 1. AIC values corresponding to the various ARMA(*p*,*q*) models for the monthly ENSO index. The lines correspond to *p* values and the columns correspond to *q* values.

ARMA	0 (q)	1	2	3	4	5	6	7	8	9	10
0 (p)	2029	1223.1	795.5	551.6	386.4	302.8	256.5	222.7	180.7	175.7	163.9
1	254.8	169.1	167.6	146.2	145.2	146.1	144.4	143.8	144.5	146.4	145.5
2	155.7	145.4	139.1	136.8	136.0	137.9	139.2	141.2	142.9	144.8	145.1
3	154.2	155.5	142.6	137.0	137.7	151.7	151.6	146.4	146.4	144.4	145.5
4	***135.2***	137.2	136.9	136.4	138.4	140.5	141.1	145.0	146.2	145.8	144.4
5	137.2	138.9	137.8	138.4	140.8	142.8	143.8	143.8	144.6	147.9	148.5
6	137.4	137.5	141.2	140.3	143.5	144.4	144.4	145.4	147.6	145.2	148.6
7	137.9	140.7	141.1	***135.9***	137.5	141.1	148.8	149.6	143.2	141.7	143.4
8	139.0	141.8	143.1	137.6	135.5	***134.0***	145.0	148.1	142.9	145.7	145.3
9	140.8	142.8	139.0	141.1	142.1	143.3	143.1	143.2	144.6	146.5	149.2
10	142.7	143.1	147.0	145.3	137.9	149.2	136.5	138.7	139.5	142.7	141.8

Table 2. RMSE for the recent 20 years of the monthly ENSO index

	ARMA(1,0)	ARMA(4,0)	ARMA(7,3)	ARMA(8,5)	TREND(1)-ARMA(4,0)	ARMA(4,0)-GARCH(1,1)	EMD-NSOR
LEAD-1	0.30	0.27	0.27	0.27	0.26	0.26	0.40
LEAD -2	0.49	0.45	0.46	0.46	0.43	0.44	0.53
LEAD -3	0.64	0.59	0.60	0.60	0.56	0.56	0.65
LEAD -4	0.76	0.71	0.72	0.72	0.67	0.67	0.76
LEAD -5	0.84	0.79	0.80	0.80	0.74	0.75	0.87
LEAD -6	0.91	0.84	0.85	0.85	0.79	0.80	0.96
LEAD -7	0.95	0.88	0.89	0.89	0.83	0.85	1.04
LEAD -8	0.99	0.91	0.91	0.91	0.86	0.88	1.11
LEAD -9	1.02	0.93	0.93	0.93	0.89	0.90	1.17
LEAD -10	1.04	0.94	0.95	0.95	0.91	0.92	1.23
LEAD -11	1.05	0.95	0.96	0.96	0.93	0.94	1.28
LEAD -12	1.06	0.95	0.96	0.96	0.95	0.95	1.33

Note that Lead-*h* presents the prediction lead time (see *h* in Eq.(7))

Table 3. Correlation between observed and forecasted values from different models for the last 20 years of the monthly ENSO index

	ARMA(1,0)	**ARMA(4,0)**	**ARMA(7,3)**	**ARMA(8,5)**	**TR1AR4**	**ARMA(4,0)-GARCH(1,1)**	**EMD**
LEAD-1	0.94	0.96	0.96	0.95	0.95	0.96	0.81
LEAD -2	0.84	0.87	0.87	0.87	0.87	0.88	0.68
LEAD -3	0.72	0.77	0.77	0.77	0.78	0.79	0.54
LEAD -4	0.59	0.64	0.64	0.64	0.66	0.68	0.37
LEAD -5	0.48	0.54	0.54	0.54	0.56	0.59	0.21
LEAD -6	0.38	0.44	0.45	0.45	0.47	0.50	0.06
LEAD -7	0.30	0.36	0.37	0.37	0.37	0.41	-0.10
LEAD -8	0.22	0.30	0.31	0.31	0.28	0.34	-0.23
LEAD -9	0.15	0.23	0.25	0.25	0.19	0.26	-0.33
LEAD -10	0.09	0.17	0.21	0.20	0.10	0.20	-0.42
LEAD -11	0.03	0.12	0.17	0.16	0.01	0.14	-0.45
LEAD -12	-0.01	0.08	0.14	0.14	-0.07	0.10	-0.47

Table 4. RMSE for the recent 20 years of monthly PDO index

	ARMA(1,0)	**ARMA(5,0)**	**ARMA(9,7)**	**ARMA(28,0)**	**Tr1AR1**	**Tr2AR2**
Lead-1	0.545	0.583	0.569	0.552	0.585	0.569
Lead -2	0.754	0.774	0.748	0.731	0.793	0.804
Lead -3	0.869	0.883	0.844	0.824	0.923	0.943
Lead -4	0.935	0.946	0.900	0.872	1.005	1.026
Lead -5	0.976	0.982	0.933	0.902	1.052	1.074
Lead -6	0.997	0.996	0.954	0.921	1.071	1.096
Lead -7	1.004	0.989	0.960	0.925	1.069	1.101
Lead -8	1.008	0.981	0.968	0.934	1.064	1.102
Lead -9	1.012	0.979	0.978	0.944	1.058	1.101
Lead -10	1.016	0.983	0.989	0.955	1.065	1.110
Lead -11	1.020	0.991	1.004	0.971	1.075	1.120
Lead -12	1.022	1.002	1.013	0.982	1.088	1.132

Table 5. Correlation between observed versus forecasted values from different models for the recent 20 years of the monthly PDO index

	ARMA(1,0)	ARMA(5,0)	ARMA(9,7)	ARMA(28,0)	Tr1AR1	Tr2AR2
Lead-1	0.866	0.827	0.831	0.832	0.841	0.835
Lead -2	0.709	0.654	0.659	0.672	0.681	0.670
Lead -3	0.559	0.507	0.508	0.538	0.536	0.529
Lead -4	0.438	0.404	0.390	0.445	0.418	0.422
Lead -5	0.338	0.332	0.301	0.374	0.326	0.342
Lead -6	0.264	0.285	0.227	0.321	0.263	0.289
Lead -7	0.249	0.279	0.195	0.300	0.241	0.269
Lead -8	0.260	0.285	0.170	0.285	0.224	0.257
Lead -9	0.269	0.284	0.149	0.268	0.199	0.243
Lead -10	0.272	0.270	0.132	0.250	0.163	0.222
Lead -11	0.254	0.237	0.094	0.214	0.120	0.187
Lead -12	0.231	0.191	0.055	0.180	0.065	0.147

Table 6. RMSE of the selected models for the recent 20 years of the monthly PDO index

	ARMA(5,0)	EMD	ARMA(5,0) GARCH(1,1)
Lead-1	0.583	0.807	0.602
Lead-2	0.774	0.994	0.809
Lead-3	0.883	1.156	0.929
Lead-4	0.946	1.257	0.990
Lead-5	0.982	1.327	1.017
Lead-6	0.996	1.352	1.027
Lead-7	0.989	1.337	1.024
Lead-8	0.981	1.324	1.020
Lead-9	0.979	1.327	1.018
Lead-10	0.983	1.338	1.021
Lead-11	0.991	1.350	1.029
Lead-12	1.002	1.360	1.045

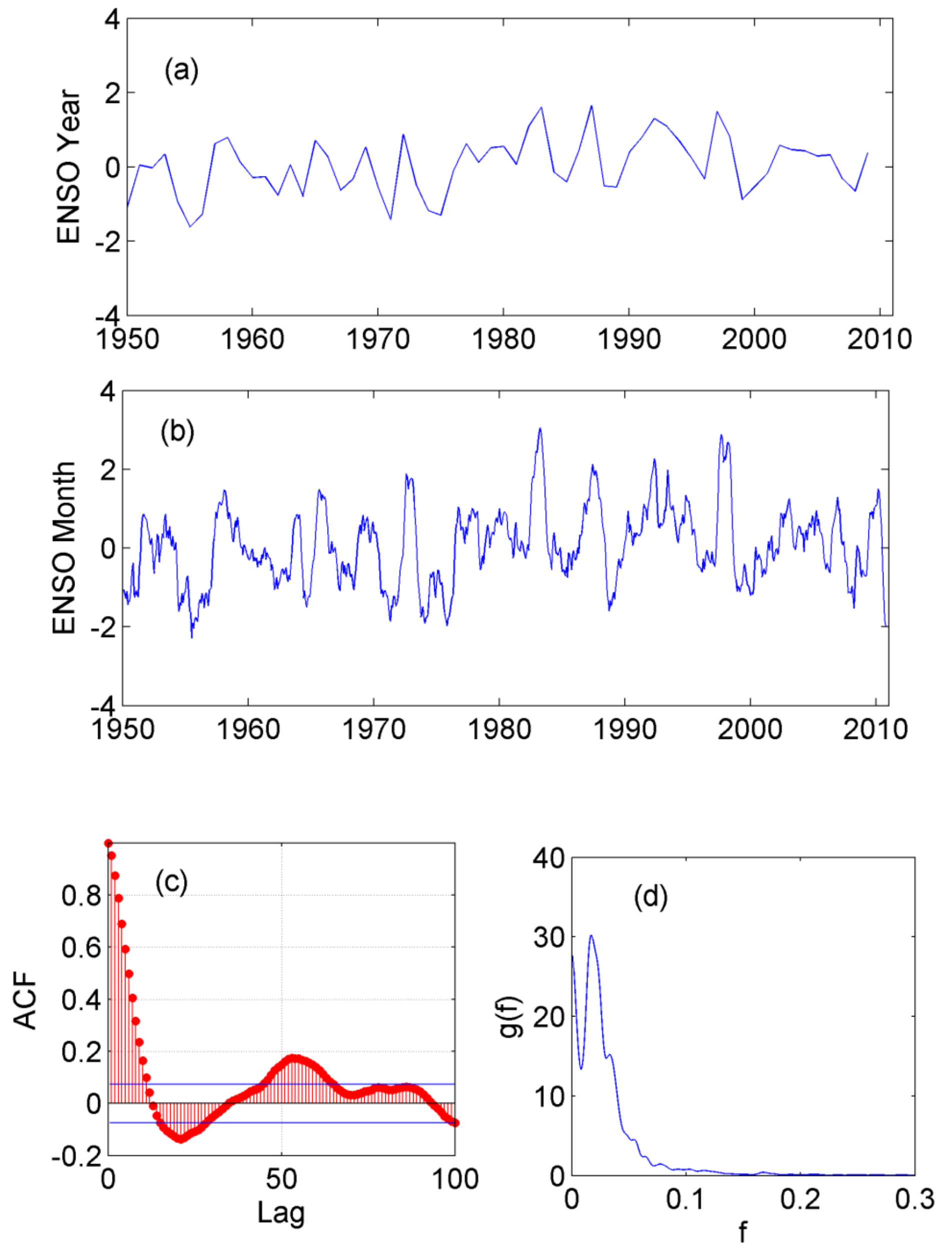

Figure 1. Annual (a) and monthly (b) ENSO time series as well as its autocorrelation function (ACF) (c) and spectral density (d) of monthly ENSO index. Note that g(*f*) presents the smoothed sample spectral density at frequency *f* (see Salas et al. 1980)

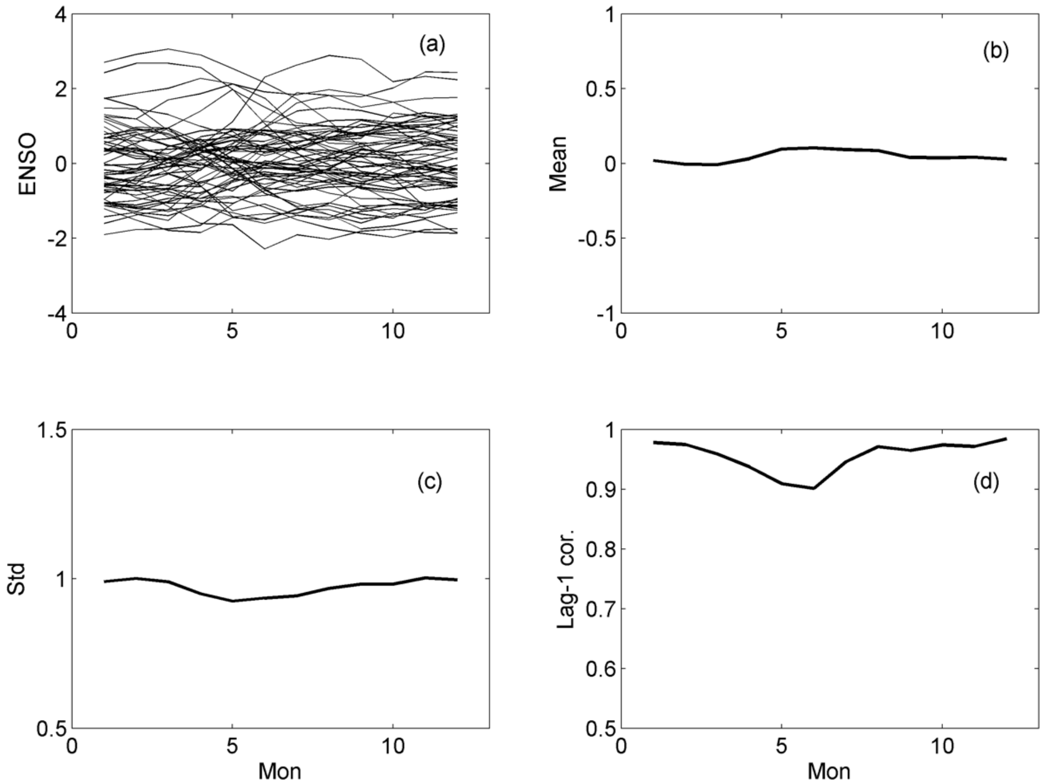

Figure 2. Seasonal variations of time series and statistics for the monthly ENSO index. (a) spaghetti plot of time series for each year and (b)-(d) monthly statistics.

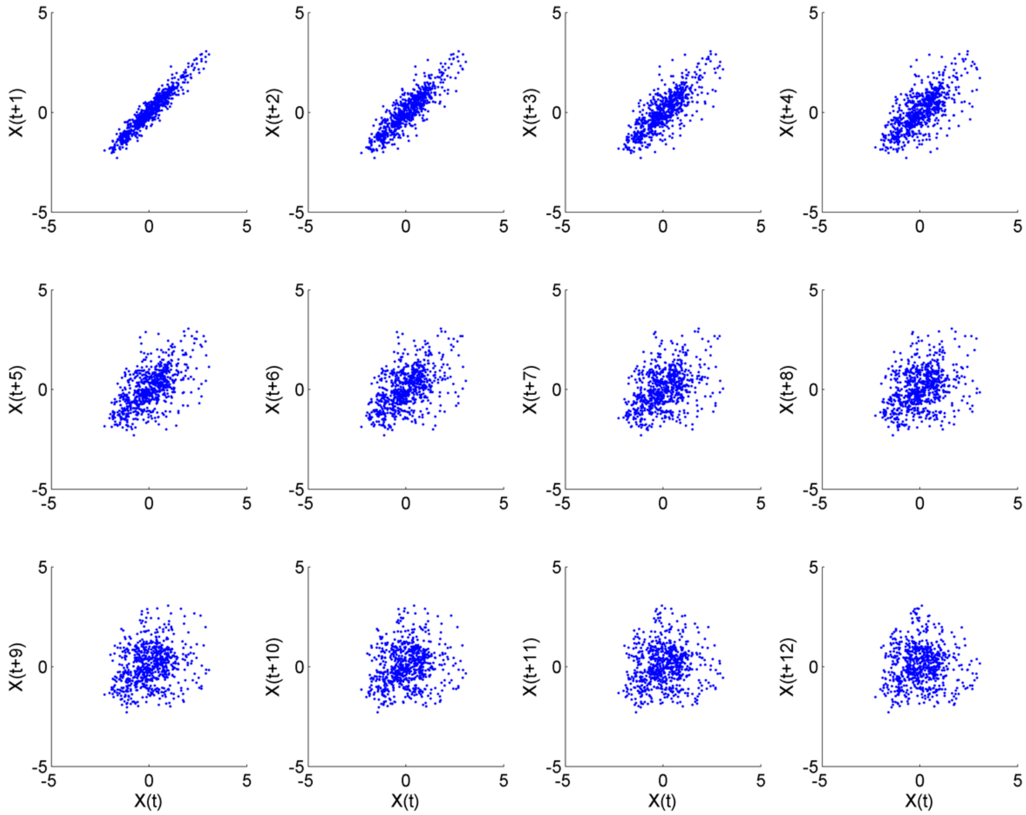

Figure 3. Scatter plots of the monthly ENSO X_t and X_{t+h} , h=1,…,12

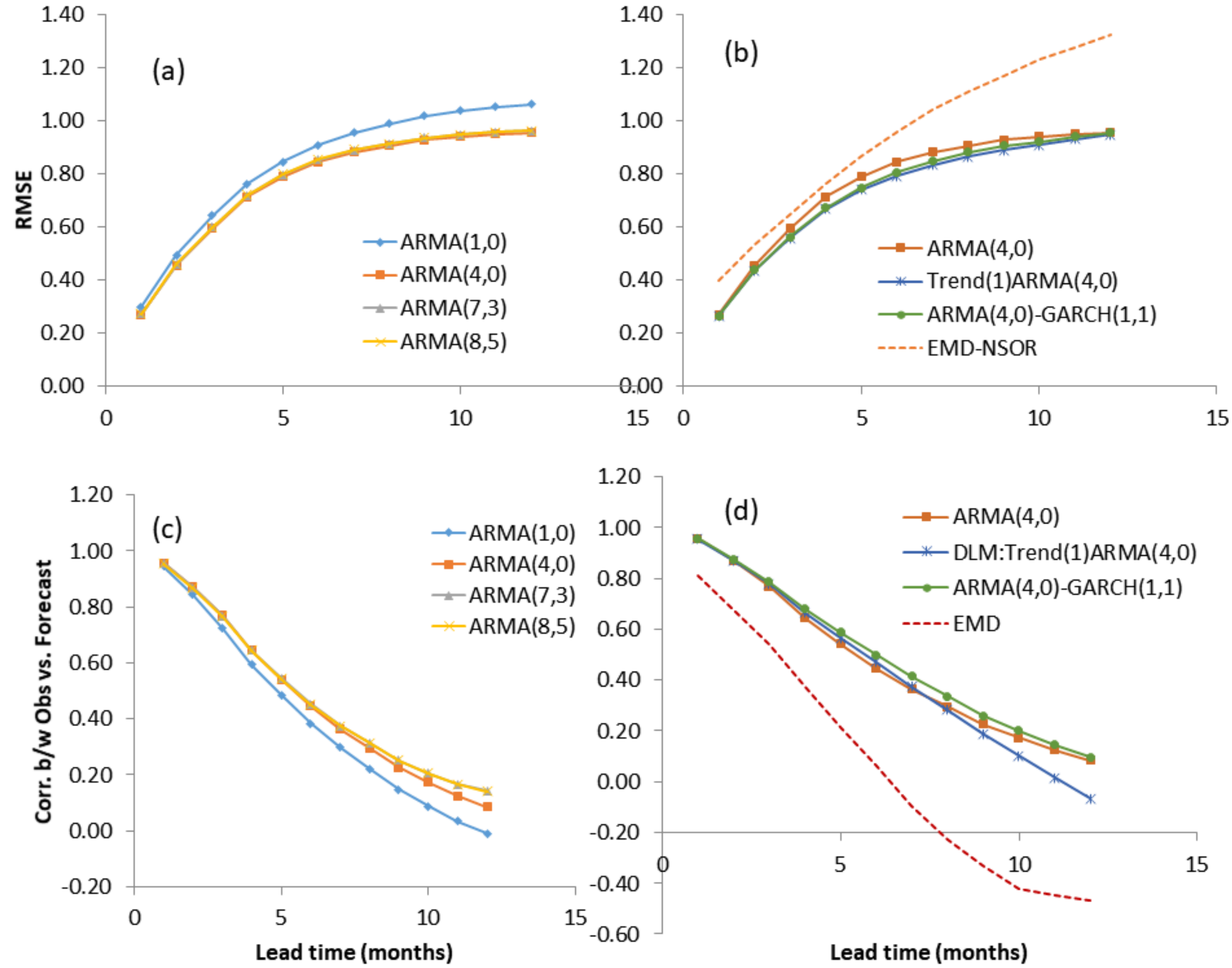

Figure 4. Performance measurements of the observed versus forecasted values for the last 20 years (1990-2009) of the monthly ENSO index for (a) RMSE of ARMA(*p*,*q*) models as ARMA(1,0), ARMA(4,0), ARMA(7,3), and ARMA(8,5);(b) RMSE of the selected models as ARMA(4,0), Trend(1)-ARMA(4,0), ARMA(4,0)-GARCH(1,1), and EMD-NSOR; (c) correlation of ARMA(*p*,*q*) models; (d) correlation of the selected models as in the panel (b). Note that the x-axis presents the lead time (*h*).

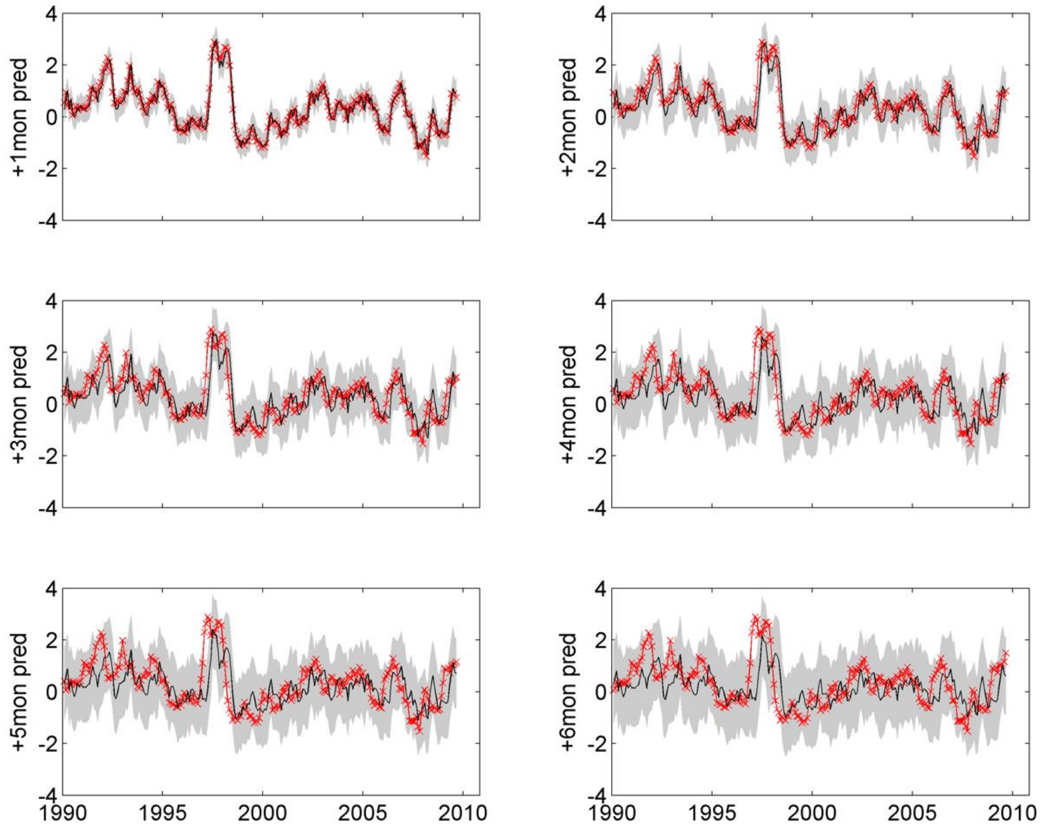

Figure 5. Forecasting the monthly ENSO index using ARMA(4,0) model for lead time *h*=1,…,6 months and for the last 20 years (1990-2009). Note that the red-cross line represents the observations and the black solid line represents the mean prediction while the gray regions show the 95 percent upper and lower limits for the mean prediction.

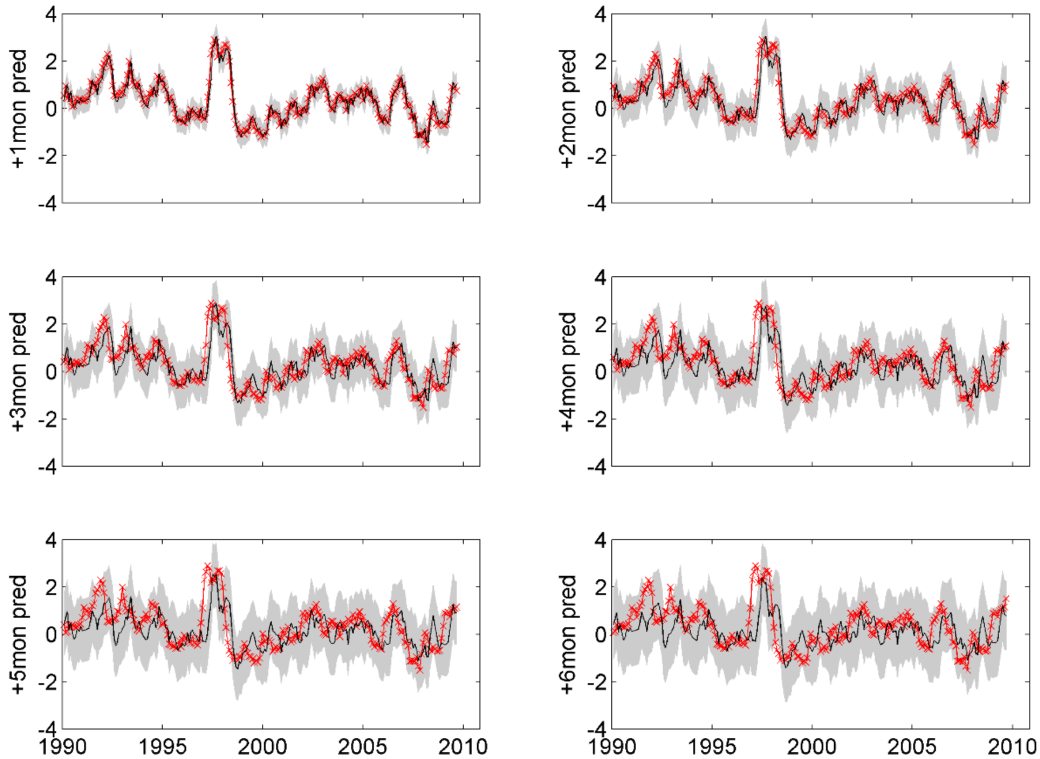

699
700 Figure 6. Same as Figure 5 but using ARMA(8,5) model.

701

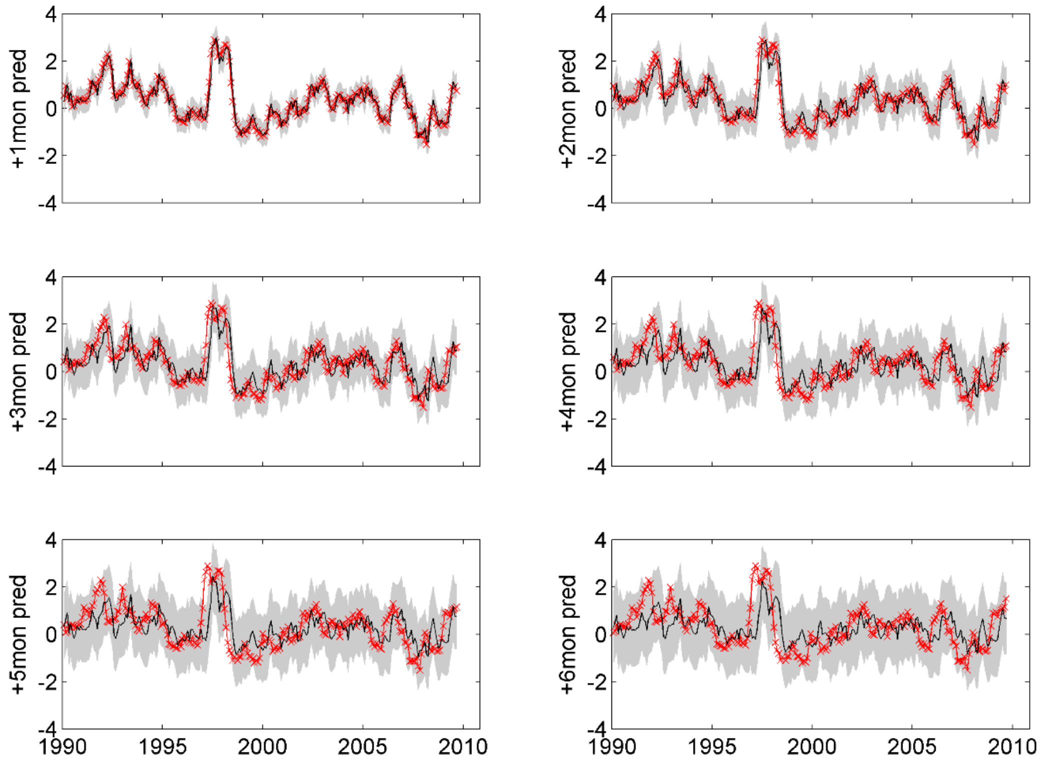

702
703 Figure 7. Same as Figure 5 but using Trend(1)-ARMA(4,0) model.

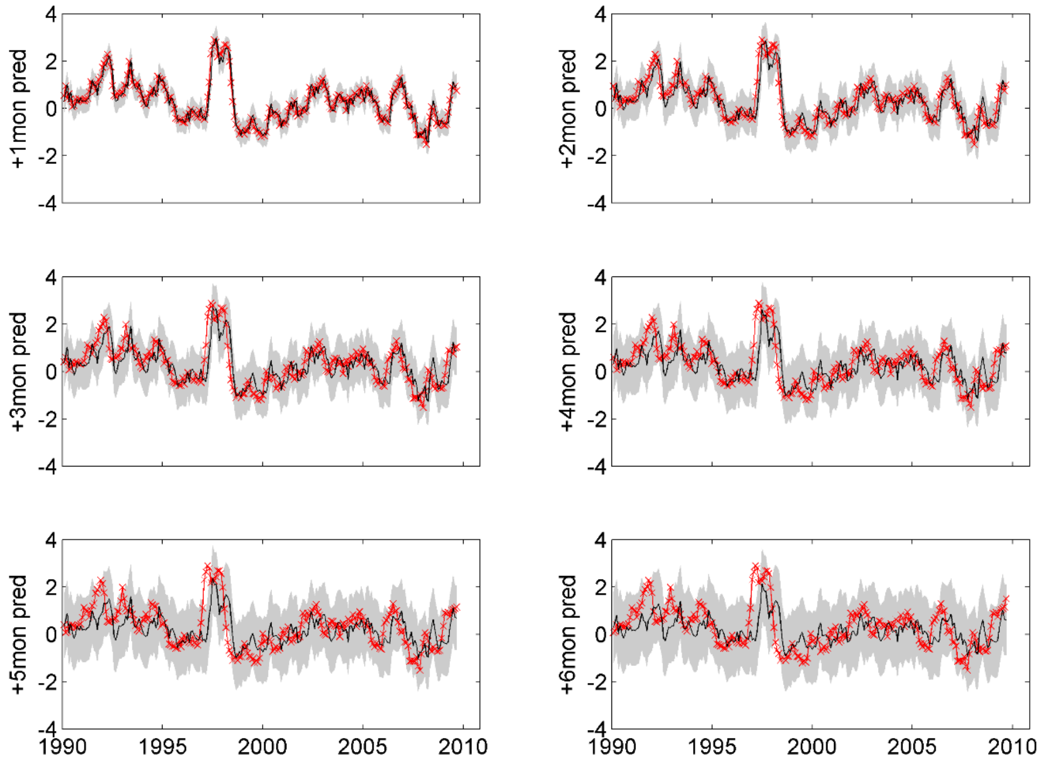

704
705 Figure 8. Same as Figure 5 but using ARMA(4,0)-GARCH(1,1) model.

706

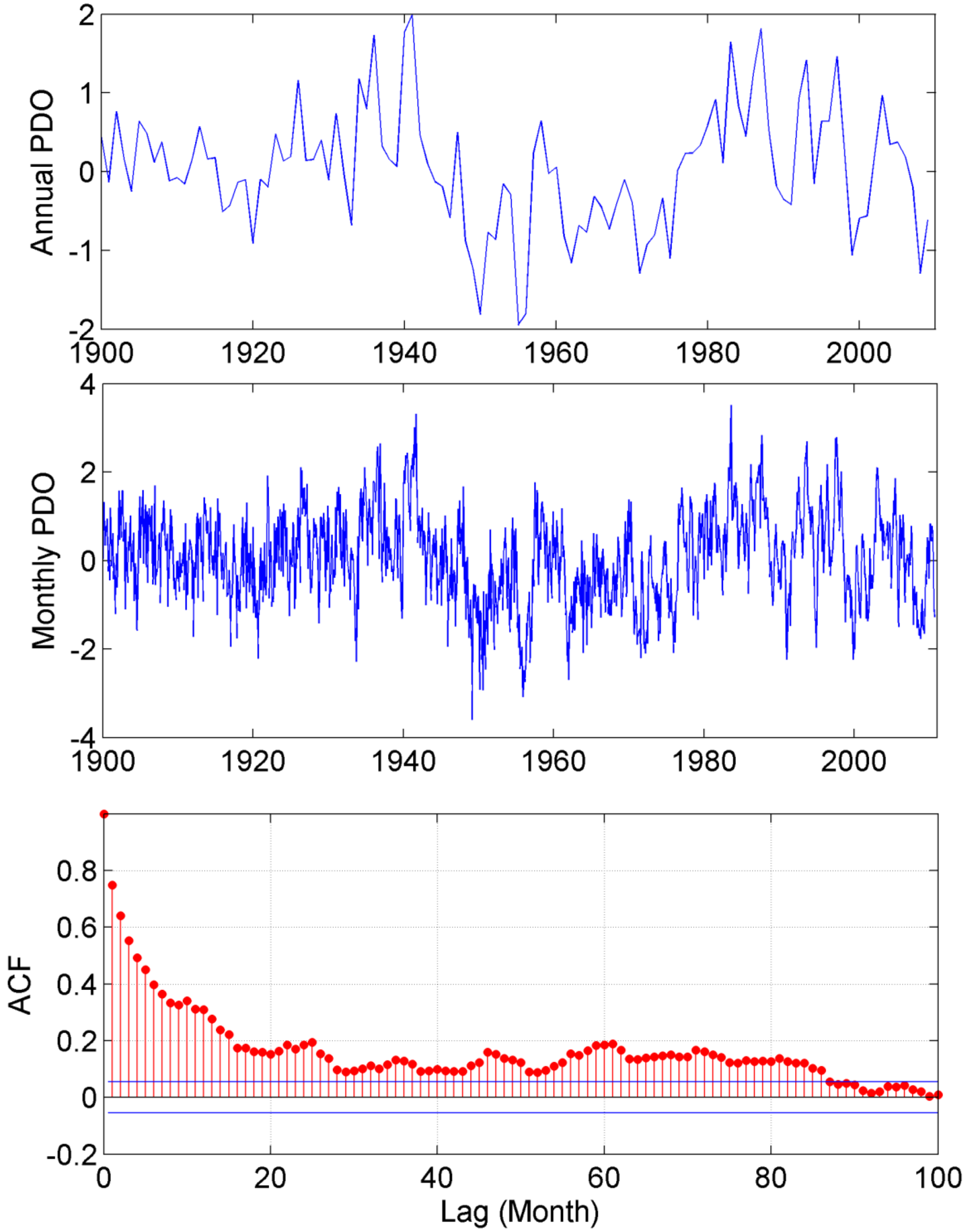

Figure 9. Annual (a) and monthly (b) PDO time series as well as its autocorrelation function (ACF) (c) of monthly ENSO index.

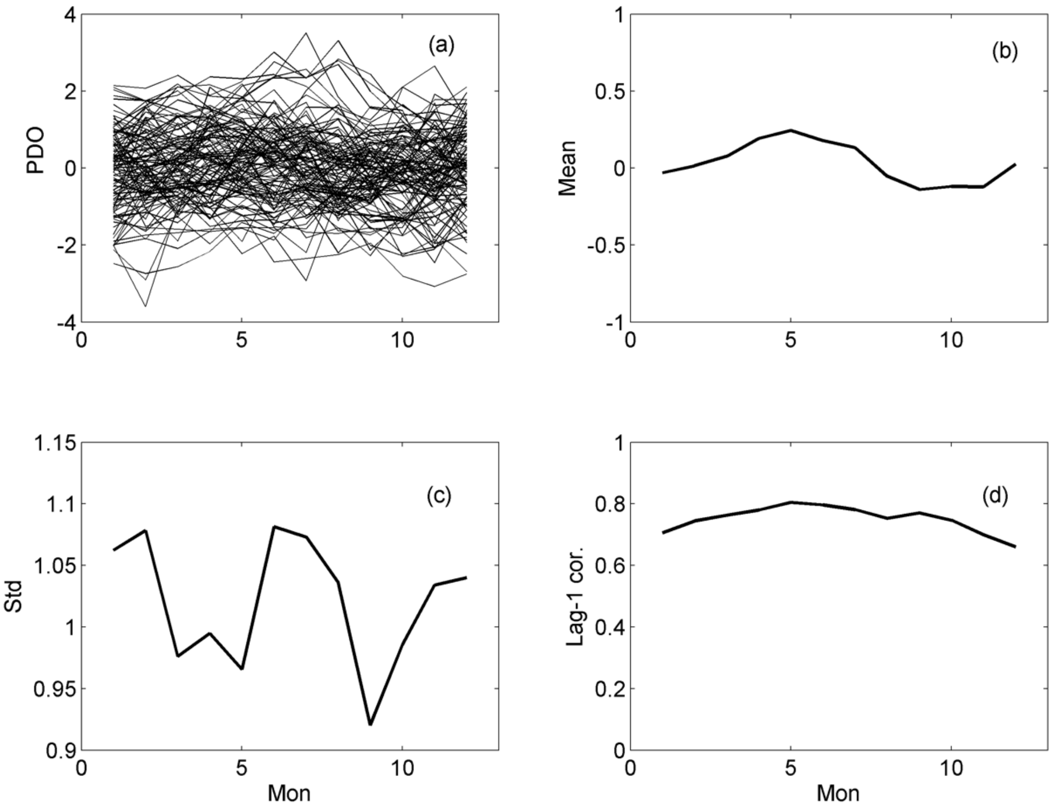

Figure 10. Seasonal variations of time series and statistics for the monthly PDO index. (a) spaghetti plots of time series for each year and (b)-(d) monthly statistics.

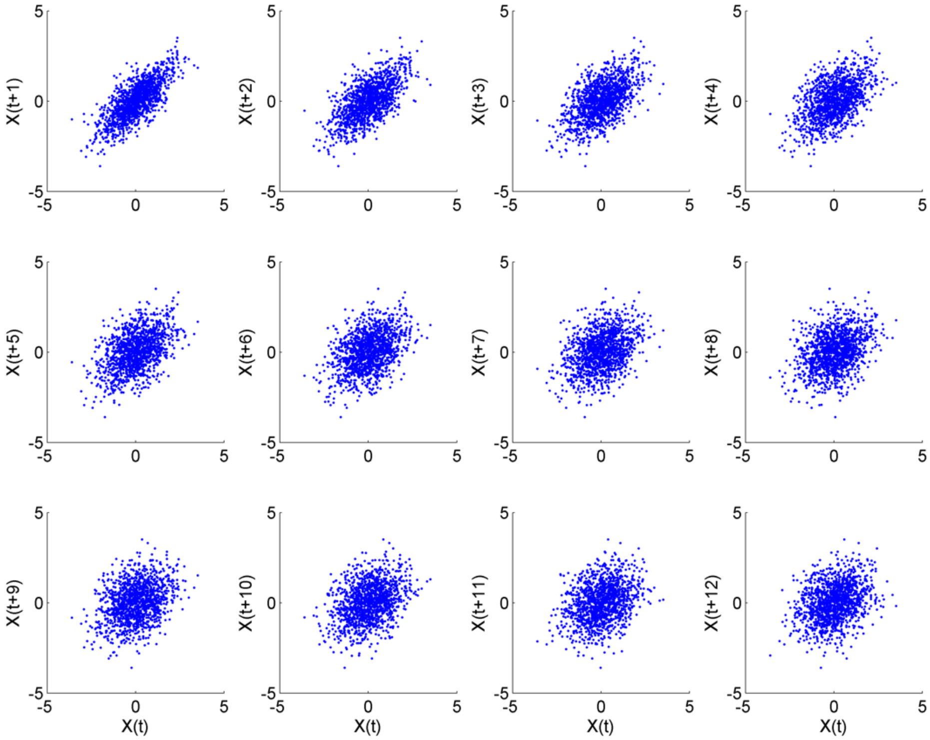

Figure 11. Scatter plots of the monthly PDO index, X_t and X_{t+h}, h=1,…,12

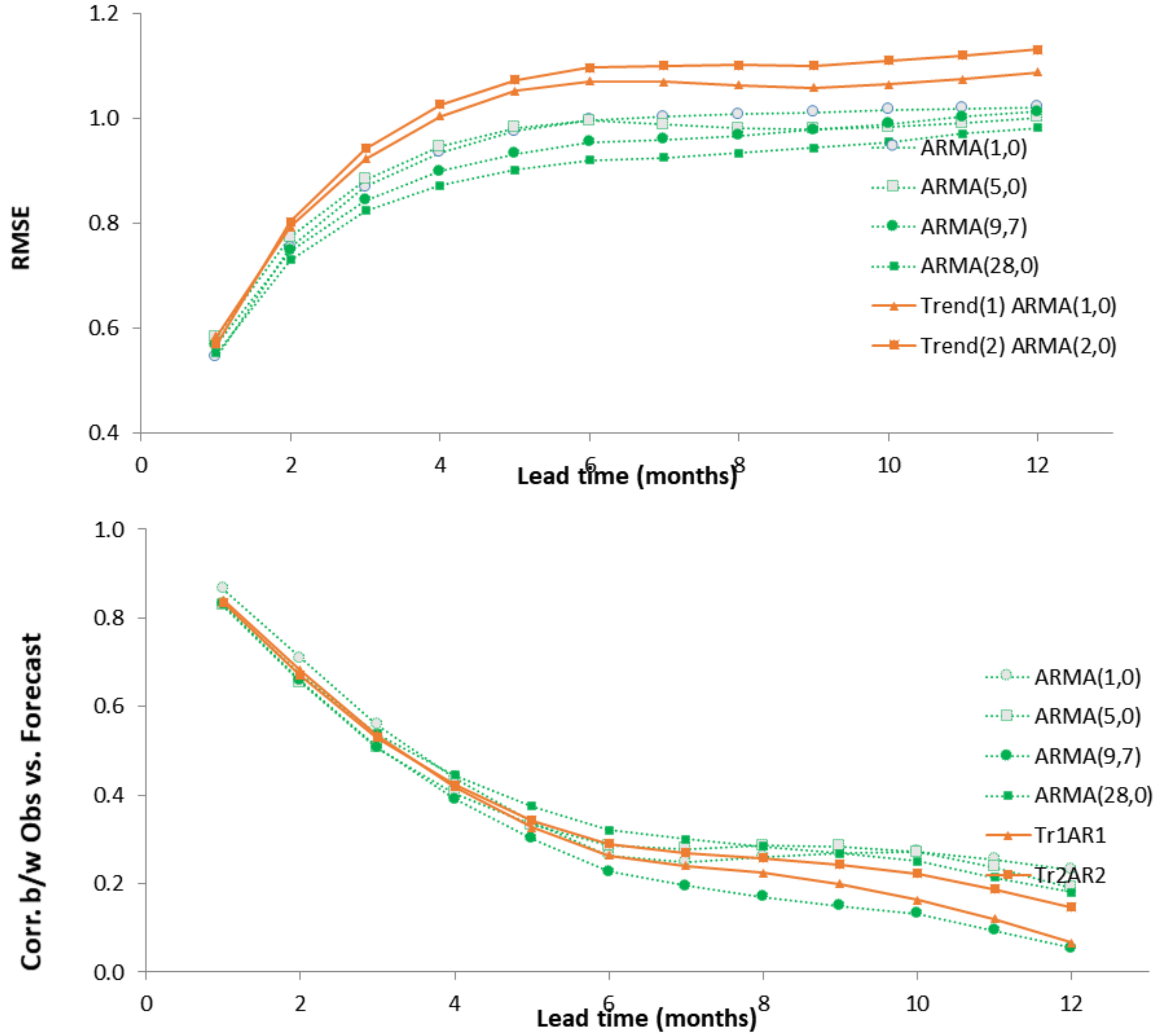

Figure 12. RMSE (top) and correlation between the observed and forecasted values of the monthly PDO index for the recent 20 year (1990-2009) with different time series models

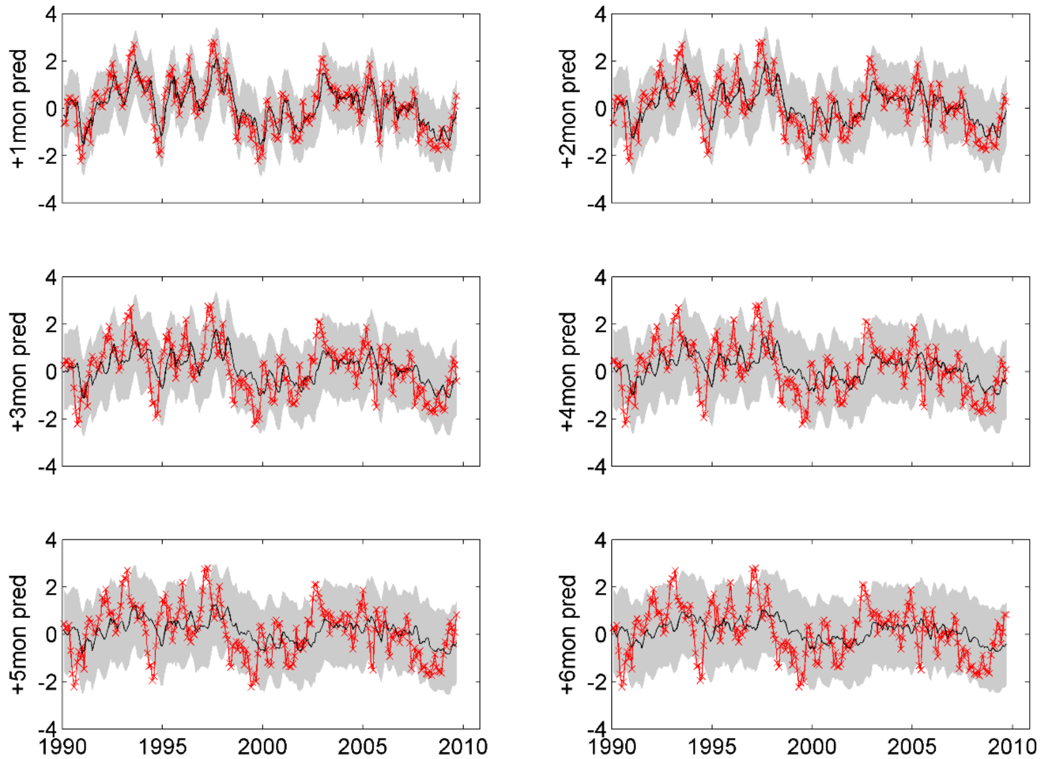

Figure 13. Forecasting the monthly PDO index using ARMA(9,7) model for lead time h=1,…,6. Note that the red-cross line represents the observation and the black solid line represents the mean prediction while the gray regions show 95 percent upper and lower limit from the mean prediction.

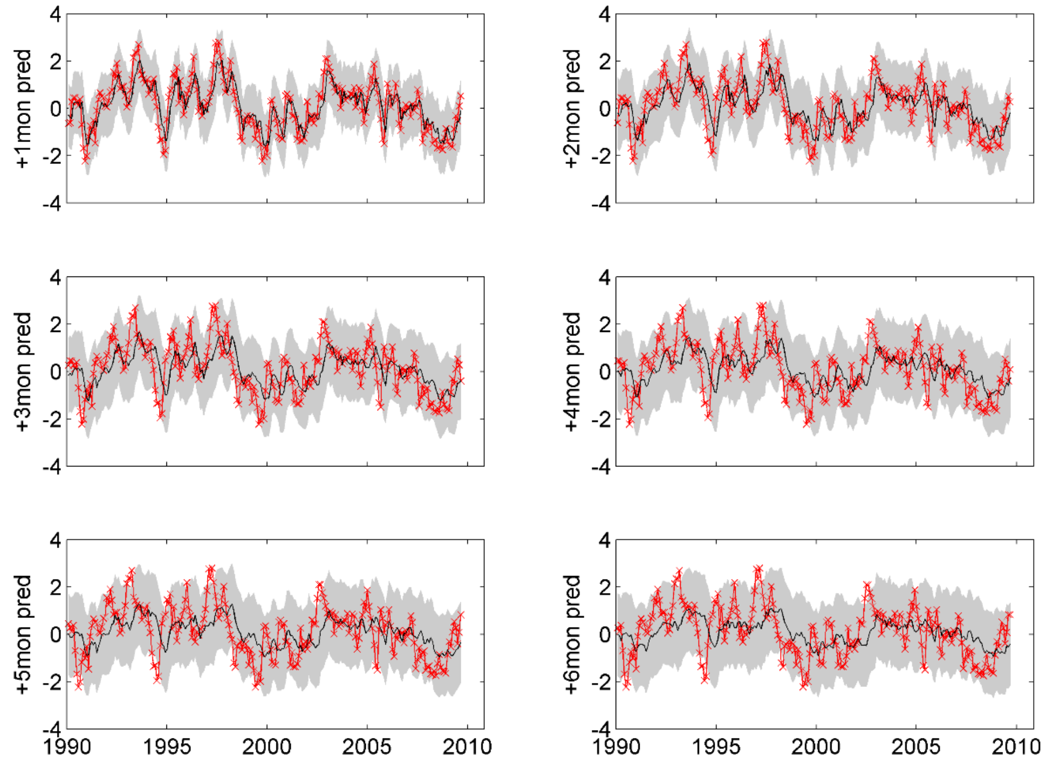

Figure 14. Same figure as Figure 5 but using ARMA(28,0) model.

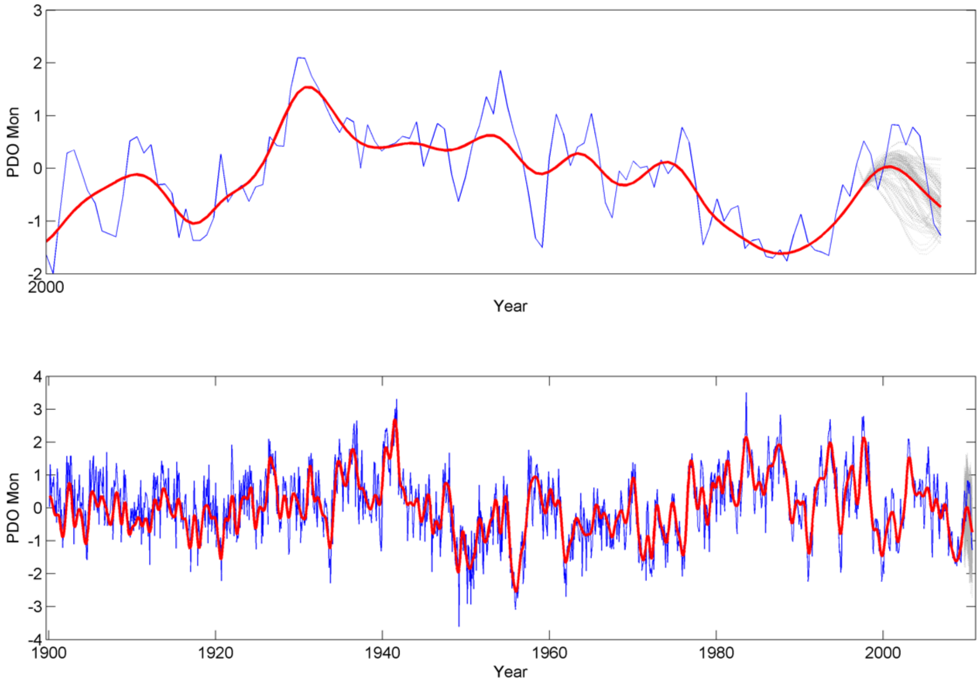

Figure 15. Last 12 months Extension of monthly PDO index with EMD-NSOR model. (1) Thin solid line represents the observations; (2) thick solid line shows the selected IMF components except the last 12 months and the mean of the generated 200 realizations for the last 12 months; and (3) dotted gray lines represent the 200 realizations of only the selected components (top panel) and of all components (bottom panel).